frontiers in Marine Science

ORIGINAL RESEARCH
published: 17 July 2018
doi: 10.3389/fmars.2018.00248

Impact of the Major Baltic Inflow in 2014 on Manganese Cycling in the Gotland Deep (Baltic Sea)

Olaf Dellwig[1], Bernhard Schnetger[2], David Meyer[3], Falk Pollehne[4], Katharina Häusler[1] and Helge W. Arz[1]*

[1] Marine Geology, Leibniz Institute for Baltic Sea Research Warnemünde (IOW), Rostock, Germany, [2] Microbiogeochemistry, Institute for Chemistry and Biology of the Marine Environment, Carl-von-Ossietzky University of Oldenburg, Oldenburg, Germany, [3] Marine Chemistry, Leibniz Institute for Baltic Sea Research Warnemünde (IOW), Rostock, Germany, [4] Biological Oceanography, Leibniz Institute for Baltic Sea Research Warnemünde (IOW), Rostock, Germany

The deep basins of the Baltic Sea, including the Gotland and Landsort Deeps, are well-known for the exceptional occurrence of sedimentary Mn carbonate. Although the details of the mechanisms of Mn carbonate formation are still under debate, a close relationship with episodic major Baltic inflows (MBIs) is generally assumed, at least for the Gotland Basin. However, the few studies on Mn cycling during MBIs suffer from a limited temporal resolution. Here we report on Mn dynamics in the water column and sediments of the Gotland Deep following an MBI that entered the Baltic Sea in December 2014. Water column profiles of dissolved Mn were obtained at a monthly to bi-monthly resolution between February 2015 and March 2017 and revealed an impact of the MBI on the Gotland Deep bottom waters beginning in March 2015. Water column profiles and budget estimates provided evidence for remarkable losses of dissolved Mn associated with the enhanced deposition of Mn oxide particles, as documented in sediment trap samples and surface sediments. In July 2015, subsequent to the nearly full oxygenation of the water column, clear signals of the re-establishment of bottom water anoxia appeared, interrupted by a second inflow pulse around February 2016. However, dissolved Mn concentrations of up to 40 μM in the bottom waters in June 2016 again indicated a pronounced reduction of Mn oxide and the escape of dissolved Mn back into the open water column. The absence of substantial amounts of Mn carbonate in the surface sediments at the end of the observation period suggested that the duration of bottom water oxygenation plays an important role in the formation of this mineral. Data from both an instrumental time series and a dated sediment core from the Gotland Deep supported this conclusion. Enhanced Mn carbonate formation occurred especially between the 1960s and mid-1970s, when several MBIs caused a long-lasting oxygenation of the water column. By contrast, Mn carbonate layers were much less pronounced or even missing after single MBIs in 1993, 2003, and 2014, each of which provided a comparatively short-term supply of O_2 to the deeper water column.

Keywords: manganese oxide, manganese carbonate, euxinia, major Baltic inflow (MBI), anoxic basin, Gotland Deep, Baltic Sea

OPEN ACCESS

Edited by:
Karol Kulinski,
Institute of Oceanology (PAN), Poland

Reviewed by:
Gennadi Lessin,
Plymouth Marine Laboratory, United Kingdom
Bradley M. Tebo,
Oregon Health and Science University, United States

****Correspondence:***
Olaf Dellwig
olaf.dellwig@io-warnemuende.de

Specialty section:
This article was submitted to Coastal Ocean Processes, a section of the journal Frontiers in Marine Science

Received: *23 March 2018*
Accepted: *27 June 2018*
Published: *17 July 2018*

Citation:
Dellwig O, Schnetger B, Meyer D, Pollehne F, Häusler K and Arz HW (2018) Impact of the Major Baltic Inflow in 2014 on Manganese Cycling in the Gotland Deep (Baltic Sea). Front. Mar. Sci. 5:248. doi: 10.3389/fmars.2018.00248

INTRODUCTION

The transition metal Mn is an essential micro-nutrient for every life-form and plays a central role in photosynthesis (Davidson and Marchant, 1987; Hansel, 2017). Redox-sensitive Mn occurs in nature in the oxidation states +2, +3, and +4, thus forming an important biogeochemical electron donor and acceptor. While the formation of solid Mn^{4+} oxides is favored in the presence of O_2, dissolved Mn^{2+} dominates under reducing conditions (Burdige, 1993). Dissolved Mn^{3+} is an important intermediate occurring in the suboxic water columns and pore waters of marine and limnic systems (Trouwborst et al., 2006; Madison et al., 2011; Dellwig et al., 2012). If reducing pore waters reach supersaturation, Ca-rich rhodochrosites containing Mn^{2+} may precipitate (Middelburg et al., 1987). The crustal abundance of Mn of ∼0.08% is low compared to ∼4% of neighboring Fe (Rudnick and Gao, 2003). However, the sensitivity of Mn to changing redox promotes the formation of massive Mn deposits in modern and ancient times; including e.g., ferromanganese crusts and nodules as well as Mn ore deposits comprising oxide, carbonate, and silicate phases (Hlawatsch et al., 2002; Nyame et al., 2003; Johnson et al., 2016). In addition to such exceptional deposits, whose mechanisms of formation are still not fully understood, sedimentary Mn signatures are also used as proxy for past redox reconstructions (Pruysers et al., 1993; März et al., 2011).

Pronounced stratification is a typical feature of restricted basins, fjords, and lakes and may promote the development of anoxic or even sulfidic (euxinic) conditions, as the limited mixing results in an insufficient O_2 supply to deeper waters (Spencer and Brewer, 1971; Jacobs et al., 1985, 1987; De Vitre et al., 1988; Skei, 1988; Murray et al., 1989; Zopfi et al., 2001; Dahl et al., 2010). At the transition between the oxygenated surface and reducing bottom waters—an area referred to as the pelagic redoxcline—intense microbial activity causes pronounced dynamics and strong gradients of nutrients and redox-sensitive metals (Dyrssen and Kremling, 1990; Taylor et al., 2001; Labrenz et al., 2007). A prominent peculiarity of redoxclines is the "Mn pump," which is initiated by the microbial oxidation of upwardly migrating dissolved Mn (Mn_{diss}) to particulate Mn oxides and their subsequent reduction as they re-enter euxinic waters either by reaction with sulfide or mediated by bacteria (Yao and Millero, 1993; Neretin et al., 2003; Tebo et al., 2004). In addition to the latter reaction between Mn and sulfide, which affects the expansion of euxinic waters, Mn may also interact with the N-cycle, as postulated by Luther et al. (1997). At pelagic redoxclines, Mn oxides are further tightly coupled to Fe and P and are believed to influence productivity by retaining certain amounts of phosphate at least over longer time-scales (Dellwig et al., 2010). Finally yet importantly, Mn oxides strongly affect trace metal cycles via scavenging and thus form an important carrier between the oxic and anoxic areas of a water body (Koschinsky et al., 2003; Dellwig et al., 2010; Yigiterhan et al., 2011).

Under reducing conditions, Mn carbonate is frequently observed in marine and lacustrine sediments as for instance in the SE Atlantic, Panama Basin, Loch Fyne, and Lake Sempach (Calvert and Price, 1970; Pedersen and Price, 1982; Gingele and Kasten, 1994; Friedl et al., 1997). Unusually high amounts of Mn carbonate are also found e.g., in manganiferous black shales deposited in the geological past (Calvert and Pedersen, 1993; Huckriede and Meischner, 1996). While missing in euxinic type-localities like the Black Sea, where euxinic bottom waters prevail since ∼7,000 years (Calvert and Pedersen, 1996; Wegwerth et al., 2018), the deep basins of the Baltic Sea are the only modern settings showing comparable and even higher Mn carbonate abundances (Suess, 1979; Lenz et al., 2015; Häusler et al., 2018). Despite their manifold occurrence, the detailed pathways of Mn carbonate formation remain unclear. Minor abundances of Mn carbonate in reducing sediments or coatings on carbonate shells may be simply explained by precipitation from supersaturated pore waters (Calvert and Pedersen, 1996). In contrast, the exceptional presence of Mn carbonate in the deep areas of the Baltic Sea requires a more complex biogeochemical and physical framework including e.g., fundamental changes in redox conditions (Huckriede and Meischner, 1996; Lepland and Stevens, 1998; Heiser et al., 2001; Lenz et al., 2015; Häusler et al., 2018). As modern type localities for intense Mn authigenesis and the formation of sedimentary Mn carbonate (Ca-rich rhodochrosite), these deeps may therefore also serve as modern analogs for sediments deposited in ancient epicontinental seas comprising manganiferous black shales and phosphorite-Mn carbonate ores (Hein et al., 1999; Jenkyns, 2010).

Although long-lasting euxinia is considered to have been characteristic of the Holocene Thermal Maximum and Medieval Climate Anomaly (e.g., Zillén et al., 2008; Jilbert and Slomp, 2013; Hardisty et al., 2016), data derived from the increased temporal resolution of (sub-)recent sedimentary records and instrumental time series suggest the occurrence of fundamental redox changes at annual to decadal scales (Neumann et al., 1997; Lenz et al., 2015; Häusler et al., 2018). Stratification of the water column fosters the development of euxinia and Black-Sea-like characteristics of the water column, such as strong bottom water Mn_{diss} enrichments, whereas irregular inflows of North Sea waters can result in the complete oxygenation of the deep basins of the Baltic Sea (Nausch et al., 2003). During these major Baltic inflows (MBIs), considerable amounts of Mn oxides are deposited on the seafloor, where, following the restoration of reducing conditions, they are presumably transformed into Mn carbonates (Huckriede and Meischner, 1996). However, a comparison of an instrumental water column time series with a sub-recent sediment record from the Gotland Basin suggested that MBIs do not necessarily result in the formation of pronounced Mn carbonate layers (Heiser et al., 2001). Rather than single MBIs, Häusler et al. (2018) identified slight bottom-water oxygenation lasting for several years as an important prerequisite of Mn carbonate formation in the Landsort Deep. In addition to experimental approaches that focus on the possible physicochemical mechanisms of Mn carbonate formation, including microbial mediation, detailed field studies during a MBI may shed light on the remarkable Mn authigenesis in the Baltic Sea. Unfortunately, studies on Mn cycling during past MBIs are extremely rare and suffer from a limited temporal resolution (Brügmann et al., 1998; Pohl

and Hennings, 1999; Turnewitsch and Pohl, 2010). However, a recent MBI entering the Baltic Sea in December 2014 (Mohrholz et al., 2015) provided the unique opportunity to follow the Mn dynamics in the Gotland Basin during an oxygenation event in detail. Water samples taken at monthly to bi-monthly intervals between February 2015 and March 2017 allowed an evaluation of Mn dynamics during the progressive oxygenation of the water column. Suspended particulate matter from a sediment trap as well as pore water samples of eight short cores were used to obtain Mn budget estimates and thus to draw conclusions on water body displacement and potential basin-internal Mn cycling. Finally, the Mn signatures of the surface sediments obtained between May 2015 and March 2017, a dated sediment core covering the past ∼70 years and instrumental water column time series are discussed in terms of the environmental conditions favoring present and past Mn carbonate formation.

MATERIALS AND METHODS

Study Site

The Baltic Sea is a brackish marginal sea comprising several basins separated by narrow sills and channels. The most prominent basins in the Baltic Proper are the Landsort Deep (∼459 m water depth), a relatively steep and narrow trench (Häusler et al., 2018), and the Gotland Basin (∼249 m water depth), with the largest areal extension and a comparatively flat center (**Figure 1**). In addition to a gradient of decreasing salinity toward the north, the water column of the Baltic Sea is permanently stratified due to the intrusion of saline waters from the North Sea and riverine freshwater inputs. The resulting restriction of vertical water-mass exchange in the deeper basins promotes a severe O_2 deficiency and the accumulation of sulfide in bottom waters (Matthäus et al., 2008).

Strong saltwater inflows from the North Sea, so-called MBIs (e.g., Matthäus and Franck, 1992), while irregular in their occurrence, enable the renewal and oxygenation of the Baltic's bottom waters. MBIs depend on certain meteorological conditions, including strong easterly winds leading to a below-normal sea level and subsequently longer-lasting westerly winds (Schinke and Matthäus, 1998). The frequency of MBIs reaching the deep basins is significantly reduced since the 1980s, possibly due to a shift in the large-scale meteorological conditions over the North Atlantic Region (Hurrell, 1995; Matthäus and Schinke, 1999; Meier and Kauker, 2003). Together with the increasing eutrophication of the Baltic Sea, especially since ∼1950, the reduced deep-water renewal has provoked the expansion of hypoxic areas (O2 <2 mL L^{-1}; Diaz and Rosenberg, 2008; Carstensen et al., 2014; Gustafsson et al., 2017).

Sampling and Sample Preparation

The samples used in this study were obtained close to the IOW monitoring station 271 (identical to station code BY15), in the central eastern Gotland Basin, during 25 cruises between 2006 and 2017 (**Table 1**). In addition, two surface sediment samples from sites MUC OD (211 m water depth) and TrKl04 (151 m water depth) were taken during Cruise POS492 in October 2015 (**Figure 1**). With the exception of pump-CTD (Strady et al., 2008) usage during cruise POS492, water column samples were obtained by a conventional CTD bottle rosette. Eight sediment cores were obtained with a multicorer device (MUC) and the pore water extracted using rhizon samplers (Seeberg-Elverfeldt et al., 2005). Samples for the determination of total dissolved Mn (Mn_{diss}) in the water column were filtered through 0.45-μM syringe filters (SFCA), whereas pore water filtration was not necessary because of a rhizon pore width of 0.1 μm. Samples for dissolved reactive Mn (dMn_{react}) were treated after Schnetger and Dellwig (2012). Water column and pore water samples were acidified to 2 vol% with concentrated HNO_3 and stored cool in acid-cleaned 2-mL reaction tubes. For sulfide analyses, 2 mL of water was fixed in 2-mL reaction tubes containing 20 μL of a 20% Zn acetate solution.

Water column samples of ∼2 L were filtered through 0.4-μm polycarbonate membrane filters for the determination of particulate Mn (Mn_{part}) in suspended particulate matter (SPM). The filters were rinsed with 60 mL of 18.2-MΩ water to remove salt and then dried at 40°C for 48 h. Time-integrated SPM samples were also obtained using a classical cone-shaped automated Kiel sediment trap with a sampling area of 0.5 m^2 (Zeitzschel et al., 1978) positioned in the central Gotland Deep (57°17.95N; 20°14.10E) at a water depth of 186 m. Sediment trap samples were recovered at a temporal resolution of 10–15 days between February 2015 and March 2017. The solid material was washed with 18.2-MΩ water and freeze-dried. A small sample aliquot was removed for scanning electron microscopy-energy dispersive X-ray spectroscopy (SEM-EDX) inspection and the remainder homogenized using an agate mortar. Sediment samples from MUC casts were sliced in intervals of 0.5–1 cm, stored frozen in Petri dishes, freeze-dried, and finally homogenized in an agate ball mill after separation of a SEM-EDX aliquot. For all solid materials, acid digestions were prepared using a HNO_3-HF-$HClO_4$ mixture in closed Teflon vessels heated to 180°C for 12 h. After evaporation of the acids to near dryness, the residues were re-dissolved, fumed off three times with 2 mL of 1+1 HCl, and finally diluted with 2 vol% HNO_3 to a volume of 50 mL (4 mL for SPM samples).

Dry bulk densities (DBDs) were estimated by dividing the weight of the dried samples by the volume of the wet samples (Brady, 1984). One short core from the MUC cast obtained in August 2012 was split lengthwise (Häusler et al., 2018) and used for X-ray fluorescence (XRF) scanning.

Analytical Methods

O_2 concentrations in the water column were determined using a SBE 911plus CTD (Sea-Bird) equipped with free-flow bottles (Hydro-Bios).

Mn_{diss} in the water column and pore waters was measured after 2-fold dilution of the samples with 2 vol% HNO_3, by inductively coupled plasma optical emission spectrometry (ICP-OES; iCAP 6300 Duo/iCAP 7300 since autumn 2016, Thermo Fisher Scientific), using external matrix-matched calibration and Sc as the internal standard. Precision (1.2%) and trueness (0.1%) were determined using 2-fold diluted international reference

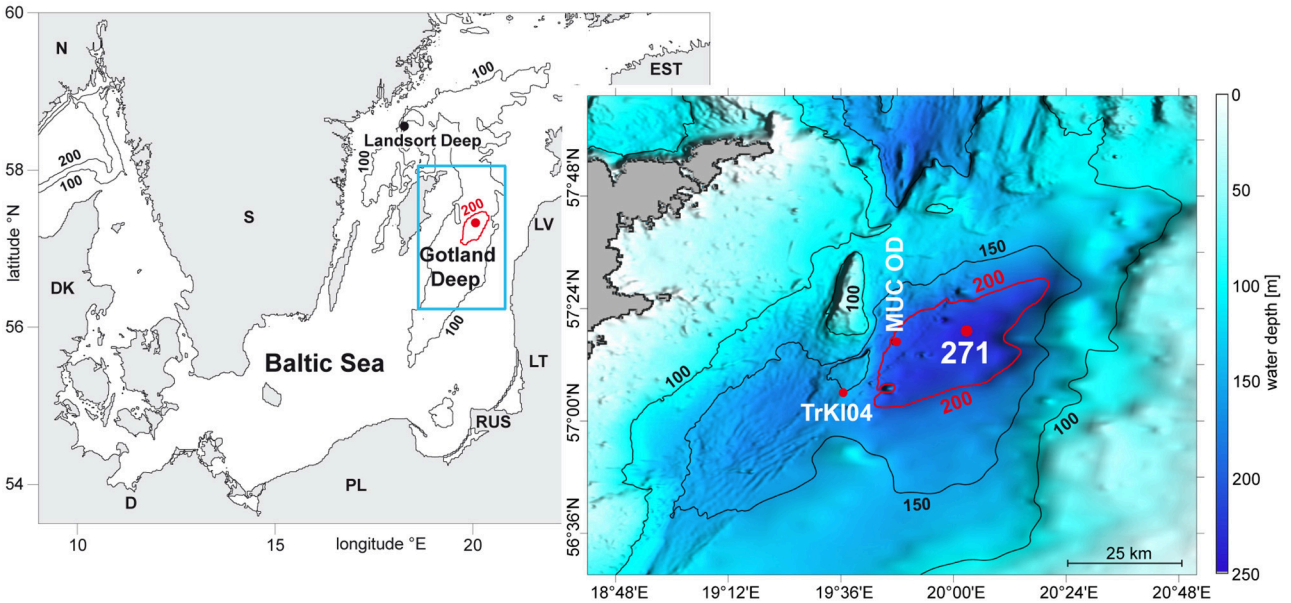

FIGURE 1 | Maps showing main sampling station 271 as well as the surface sediment stations MUC OD and TrKl04 in the central Gotland Basin. The bathymetry is described by the EMODnet Bathymetry Consortium (2016).

material SLEW-3 (National Research Council Canada) spiked with Mn.

The numerical rate estimation from concentrations model (REC; Lettmann et al., 2012) was used to estimate Mn_{diss} fluxes in the top 5 cm of the pore waters. Sediment porosity was calculated from the DBDs using an average grain density of 2.7075 g cm^{-3}. The sedimentary diffusion coefficients of Mn (Boudreau, 1997; Berg et al., 1998; Schulz, 2006) were corrected for porosity as well as temperature and salinity as determined from the CTD casts. For details, see Häusler et al. (2018).

Total sulfide concentrations in the pore water and water column samples were measured spectrophotometrically after the method of Cline (1969).

The concentrations of Al, Ca, and Mn in the acid digestions of sediments, sediment trap material, and SPM were measured by ICP-OES (iCAP 6300 Duo and iCAP 7300 since autumn 2016, Thermo Fisher Scientific) using external calibration and Sc as internal standard. The precision and trueness of the international reference material SGR-1b (USGS) were better than 2.% and −4.5%, respectively. The Pb content of the samples was determined from the same acid digestions by Q-ICP-MS (iCAP Q, Thermo Fisher Scientific) using external calibration and Ir as the internal standard. The precision and trueness of the international reference material SGR-1b (USGS) were 3.7 and −2.6%, respectively. The $^{206/207}$Pb ratios in the acid digestions of the sediment samples from the August 2012 core were also determined by Q-ICP-MS (iCAP Q, Thermo Fisher Scientific). The Q-ICP-MS was equipped with a PrepFast module (ESI), which allowed online sample dilution to a final Pb concentration of ∼1 µg L^{-1}. Following the method of Hinrichs et al. (2002), the instrument was tuned to provide the best performance for the NIST standard SRM 981. Precision and trueness were 0.04 and −0.17%, respectively.

Biogenic opal in the August 2012 short core was measured by ICP-OES (iCAP 6300 Duo, Thermo Fisher Scientific) after the extraction of 50 mg of sediment with 100 mL of 1 M NaOH for 40 min at 80°C in a shaking water bath. The precision of the in-house reference material SIBER was 4%. Si concentrations were converted into those of biogenic opal based on a conversion factor of 2.38, which considered the water content of pure biogenic opal material (diatomite).

^{137}Cs and ^{241}Am activities in the sediment samples from August 2012 were determined by gamma spectrometry (Canberra) using a planar Ge-detector GX3018-7500SL and processed using GENIE 2000 3.0 and 3.1 software (Canberra Industries Inc., USA). Counting statistics for ^{137}Cs and ^{241}Am were better than 5 and 20%, respectively. Trueness was checked against the standard reference materials IAEA-384 (^{241}Am) and IAEA-385 (^{241}Am, ^{137}Cs, decay corrected; International Atomic Energy Agency).

A parallel core from the same August 2012 MUC cast was split lengthwise (Häusler et al., 2018) and analyzed for Ca, Mn, and Ti by XRF core scanning (ITRAX XRF core scanner, Cox; Croudace et al., 2006). The sediment surface was cleaned, smoothed, and covered with a special plastic foil to minimize evaporation during the measurement. The Cr-tube operated at 30 kV and 30 mA with an exposure time of 15 s per step (step size: 200 µm).

SEM-EDX (Merlin VP Compact, Zeiss/AZtecEnergy, Oxford Instruments) was used to identify the Mn mineral phases in the sediment trap material and surface sediments. After suspension of the solid material in an ultrasonic bath and filtration through

TABLE 1 | Cruises from which sample material was obtained close to the IOW monitoring station 271 (BY15), in the central Gotland Deep (PE = R/V *Prof. Albrecht Penck*, MSM = R/V *Maria S. Merian*, M = R/V *Meteor*, EZ/EMB = R/V *Elisabeth Mann Borgese*, AL = R/V *Alkor*, POS = R/V *Poseidon*, Sal = R/V *Salme*).

Cruise	Date	Position	Water depth [m]	Device
40PE0616	14 Jul 2006	57°19.05N, 20°2.47E	237	CTD
07PE0708	13 Apr 2007	57°19.54N, 20°3.17E	241	CTD
07PE0814	4 Jul 2008	57°18.46N, 20°3.90E	243	CTD
MSM12-4b	17 Sep 2009	57°19.20N, 20°3.00E	237	CTD
M86-1b	14 Nov 2011	57°18.34N, 20°4.70E	236	CTD
06EZ1215	25 Aug 2012	57°19.29N, 20°8.15E	241	CTD/MUC
EMB95	10 Feb 2015	57°19.18N, 20°2.99E	238	CTD
AL451	3 Mar 2015	57°19.21N, 20°2.94E	234	CTD
EMB99	22 Mar 2015	57°19.19N, 20°2.84E	237	CTD
EMB100	19 Apr 2015	57°19.22N, 20°2.97E	238	CTD
EMB102	9 May 2015	57°19.24N, 20°2.86E	237	CTD
Sal2015_11	2 Jul 2015	57°19.30N, 20°3.85E	235	CTD
EMB107	21 Jul 2015	57°19.19N, 20°2.95E	237	CTD/MUC
EMB113	25 Sep 2015	57°19.20N, 20°2.90E	237	CTD
POS492	20 Oct 2015	57°19.19N, 20°2.90E	241	CTD/MUC
EMB117	11 Nov 2015	57°19.21N, 20°3.03E	238	CTD
EMB120	4 Feb 2016	57°19.20N, 20°3.05E	238	CTD
MSM51	13 Feb 2016	57°19.19N, 20°2.99E	237	MUC
EMB124	20 Mar 2016	57°19.21N, 20°3.10E	237	CTD
EMB128	15 May 2016	57°19.21N, 20°2.95E	236	CTD
AL479	9 Jun 2016	57°19.19N, 20°2.99E	238	CTD/MUC
EMB135	7 Aug 2016	57°19.05N, 20°3.11E	237	CTD
POS507	19 Oct 2016	57°18.32N, 20°4.70E	244	CTD/MUC
EMB147	12 Feb 2017	57°19.31N, 20°2.82E	236	CTD
MSM62	10 Mar 2017	57°16.83N, 20°5.87E	238	CTD/MUC

0.4-μm polycarbonate filters, the samples were fixed on Al stubs, carbon coated, and placed in a vacuum chamber. The working distance was 8.5 mm and spot analysis was done at an excitation voltage of 15 kV. Relative mineral abundances were determined by automated particle analyses, which were based on EDX element analyses of ∼2,000 particles per sample, image processing, and particle recognition. The border values for the differentiation of Mn oxide from Ca-rich Mn carbonate were: Mn >30%, Ca <6%, and Mn >30%, Ca >6%.

RESULTS

Mn Dynamics in the Water Column of the Gotland Deep Prior to the MBI of 2014

Figure 2 shows six water column profiles of dissolved and particulate Mn (Mn_{diss}, Mn_{part}), O_2, and total sulfide from the Gotland Deep at monitoring site 271 (**Figure 1**). The respective samples were taken between 2006 and 2012, during a so-called stagnation period, that is, without a substantial impact of an MBI. In July 2006, Mn_{part} was strongly enriched just above and Mn_{diss} below the redoxcline. After slightly decreasing at a water depth of around 160 m, Mn_{diss} concentrations increased again and reached a maximum of ∼26 μM in the deepest sample. Along with an upward shift of the redoxcline by ∼10 m in April 2007, Mn_{part} and Mn_{diss} enrichments were less pronounced in the suboxic waters. Below the redoxcline, Mn_{diss} remained at a nearly constant level of ∼11 μM until a sudden drop to ∼5 μM in the deepest two samples. While sulfide concentrations gradually increased with depth, to a maximum of 45 μM at 221 m, the values abruptly declined to as low as ∼2 μM just above the seafloor. In July 2008, the redoxcline occurred a few meters further upward. Mn_{diss} concentrations gradually increased with depth and remained constant at ∼10 μM below a water depth of 170 m. Sulfide concentrations also increased with water depth, reaching a maximum of 48 μM in the bottom waters. Despite lower concentrations of Mn_{part} and a bottom water sulfide level of 114 μM, the Mn_{diss} profile in September 2009 generally coincided with that of the previous cruise, in 2008. In November 2011, the sulfide concentration in the bottom waters increased to a maximum of 148 μM, while Mn_{diss} concentrations within the deeper water column remained at a similar level of ∼10 μM. In August 2012, O_2 concentrations increased strongly between water depths of 95 m and 130 m whereas the Mn_{diss} profile in deeper waters was more or less unaffected and resembled that of the previous cruises since 2008.

Mn Dynamics in the Water Column of the Gotland Deep During the MBI of 2014

Figure 3 shows O_2 and Mn_{diss} as well as available Mn_{part} and sulfide concentrations in the water column of the Gotland Deep at site 271 as determined during 18 cruises between February 2015 and March 2017. Compared to the pre-MBI profiles (**Figure 2**), the Mn_{diss} concentration during the first cruise (February 2015) was generally lower throughout the sulfidic water body. Although Mn_{diss} increased steeply, to a maximum of 6.4 μM, just below the redoxcline, its concentration in sulfidic waters gradually decreased, to 3.2 μM in the lowermost sample. Distinctly lower concentrations of sulfide, fluctuating around 20 μM, were also measured at water depths of 150–235 m. Almost 1 month later (3 March 2015), O_2 appeared in the bottom waters at concentrations ranging from 9 μM at a water depth of 208 m to 35 μM near the seafloor (231 m). In parallel, Mn_{diss} concentrations in the two deepest samples decreased to ∼1.0 μM. During the following four cruises, oxygenation of the deeper waters proceeded and Mn_{diss} was increasingly depleted. By 9 May 2015 and persisting until at least 2 July 2015, only a thin relict of the former euxinic water body remained, occurring at ∼130 m water depth. An O_2 concentration of nearly 100 μM characterized the water column from the bottom until a water depth of ∼130 m, whereas Mn_{diss} and sulfide concentrations were as low as ∼3 μM in the depth interval between 125 and 110 m.

In the same depth interval, elevated Mn_{diss} concentrations as high as 6.3, 3.4, and 2.7 μM were also determined on 21 July 2015, 26 September 2015, and 27 October 2015, respectively. The values then dropped to < 0.4 μM on 11 November 2015. Beginning with the cruise on 21 July 2015, however, the Mn_{diss} level in the bottom waters began to increase, reaching a maximum of almost 20 μM

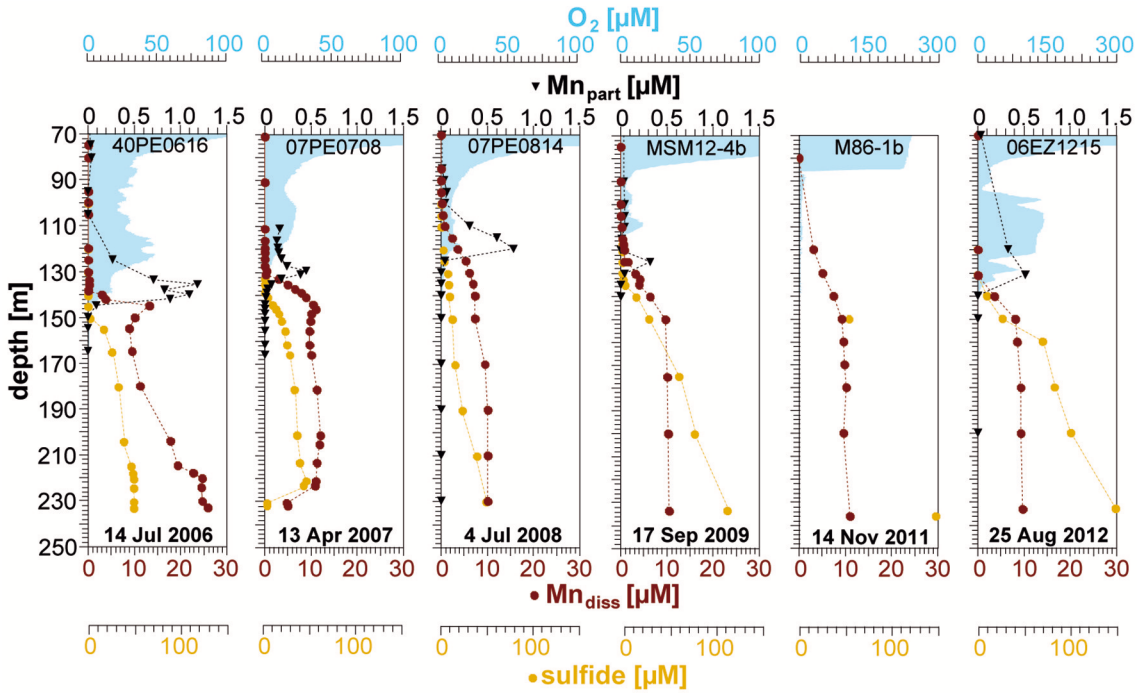

FIGURE 2 | Water column profiles of O_2, dissolved and particulate Mn, and total sulfide as determined in samples obtained from station 271 in the central Gotland Basin between 2006 and 2012.

in the deepest water samples in October and November 2015. Supernatant waters of the corresponding short cores contained up to 16 µM Mn_{diss} on 21 July 2015 and 25 µM Mn_{diss} on 27 October 2015. In samples from those two cruises, particulate Mn (Mn_{part}) concentrations showed two maxima, of 0.57 µM (128 m) and 2.9 µM (233 m), on 21 July 2015 and three maxima, of 0.98 µM (83 m), 0.65 µM (137 m), and 1.4 µM (231 m), in October 2015. Maximum sulfide concentrations were ∼0.8 µM, within the detection limit of the method used during both cruises.

On 4 February 2016, O_2 concentrations again increased in the bottom waters, reaching 76 µM. While Mn_{diss} ranged between 2 and 12 µM in these O_2-containing waters, the concentration in the still-anoxic overlying waters was 34 µM. A further decrease in the Mn_{diss} concentration was measured in the 20 March 2016 samples, and a continuing decline, to below ∼0.1 µM, throughout the almost entirely oxygenated water column in May 2016. Three weeks later (09 June 2016), the bottom waters again became anoxic at depths below 220 m. In these waters, Mn_{diss} was strongly enriched, reaching 40 µM in the supernatant waters of the corresponding short core. This trend of a re-establishment of bottom water anoxia was also reflected by increasing Mn_{diss} and sulfide concentrations during the remaining four cruises. Above the sulfide-containing waters, Mn_{part} was clearly enriched, both on 9 June 2016 and on 19 October 2016, showing a maximum concentration of 2.4 µM. On 10 March 2017, the reducing conditions extended from the bottom to a water depth of ∼180 m and Mn_{diss} and sulfide concentrations were as high as 58 and 36 µM, respectively.

Please note that Mn_{diss} represents the sum of dissolved Mn^{2+} and the intermediate Mn^{3+} species with the latter partly entirely dominating in suboxic waters (Trouwborst et al., 2006). The determination of dMn_{react} comprising mainly of Mn^{3+} (Schnetger and Dellwig, 2012) during four cruises revealed only a secondary role of Mn^{3+} under the unstable hydrodynamic conditions prevailing in the Gotland Basin (Figure S1). This finding accords with a previous study in the Baltic and Black Seas highlighting non-turbulent redoxclines as an important prerequisite for substantial Mn^{3+} accumulation (Dellwig et al., 2012).

Particulate Mn in a Sediment Trap Positioned in the Gotland Deep

Multiplying the bulk SPM fluxes of the sediment trap close to site 271 with the corresponding Mn_{part} contents allowed the calculation of Mn_{part} fluxes (Supplementary Dataset). Although the MBI reached the deepest parts of the central Gotland Basin no later than the beginning of March 2015 (**Figure 3**), Mn_{part} fluxes remained low until the end of April 2015, as determined from the sediment trap placed at a water depth of 186 m (**Figure 4**). Thereafter, a slight increase in Mn_{part} fluxes was followed by a steep rise at the end of June 2015. A malfunction of the sediment trap prevented coverage of later developments, until the end of November 2015. To estimate the Mn_{part} fluxes that might have occurred during this missing interval of the MBI, we included a dataset from an MBI in 2003 (Häusler et al., 2018). Although O_2 concentrations were slightly higher in 2003

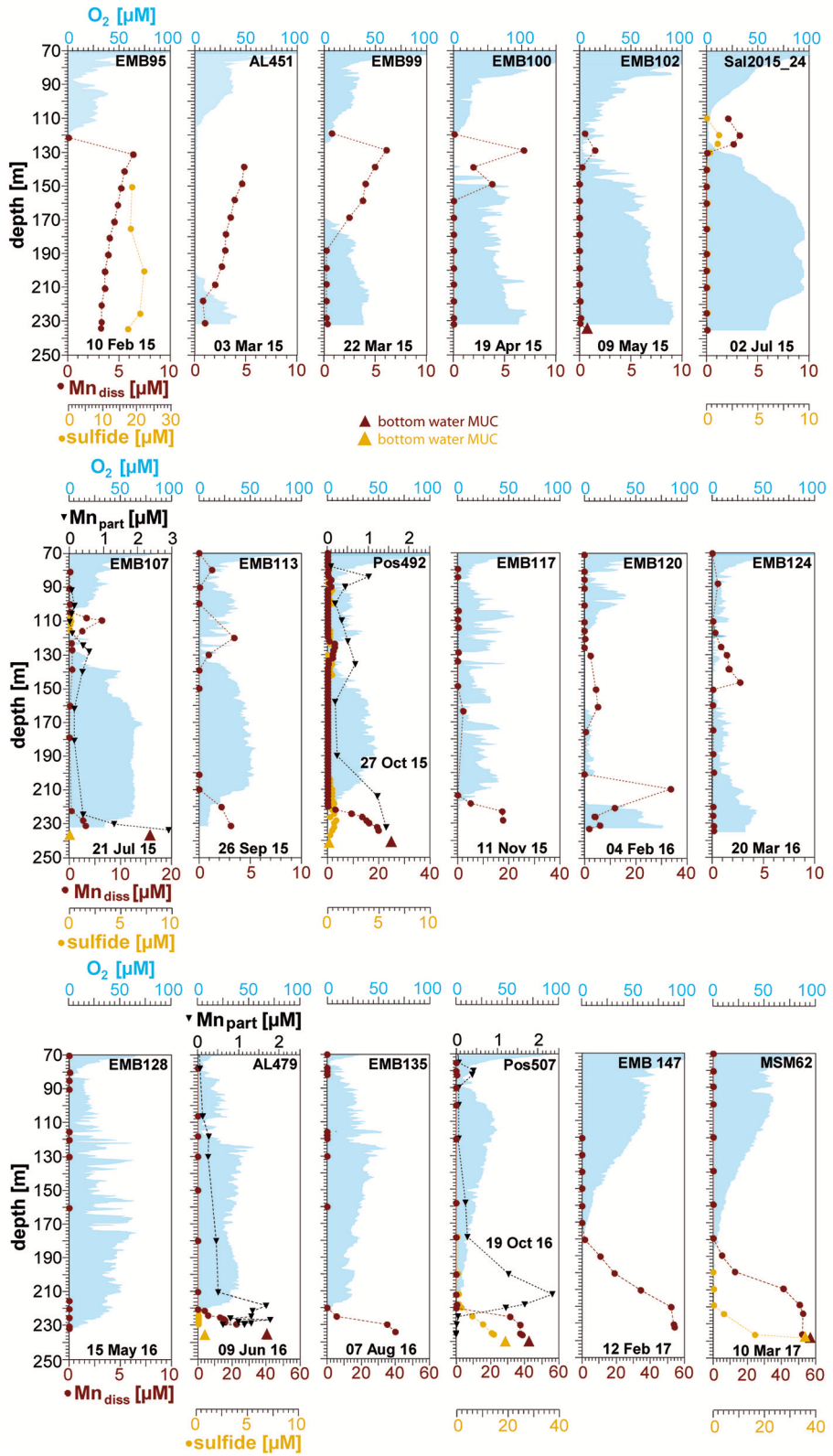

FIGURE 3 | Water column profiles of O_2, dissolved and particulate Mn, and total sulfide as determined in samples obtained from station 271 in the central Gotland Basin between February 2015 and March 2017. Large yellow and brown triangles denote sulfide and Mn_{diss} concentrations, respectively, in the supernatant water of the corresponding short cores.

than in 2015 (Figure S3), the chosen sediment trap dataset from 2003 at least represented a situation within MBI development comparable to that of 2015. Thus, the 2003 data also showed a rapid increase in Mn_{part} fluxes shortly after the onset of the MBI and a decrease to a relatively low level in the following 5 months. After the onset of a second oxygenation phase, Mn_{part} fluxes again increased steeply and strongly fluctuated until March 2017.

Surface Sediments and Pore Waters From the Gotland Deep

Eight short cores taken close to monitoring station 271 were analyzed for their sedimentary Al, Ca, and Mn contents (**Figure 5**). To eliminate dilution effects by organic matter and salt, especially in the uppermost fluffy parts, the Ca and Mn contents were normalized to the Al content. Based on the salinity of the bottom waters, the Ca contents were corrected for the pore water salt content. Because the positions of the coring locations varied between the cruises by a few nautical miles (**Table 1**), differences in the sediment records were most likely due to variable sedimentation rates. Based on a core parallelization using Pb/Al ratios indicating maximum Pb pollution between ∼1970 and 1980 (Renberg et al., 2001), in the cores from August 2012 and October 2016 older Mn enrichments occurring at a depth of ∼6 cm did not appear before 10 and 14 cm (**Figure 5** and Figure S2), respectively. Nonetheless, because all cores originated from water depths below 237 m, a comparison of the uppermost fluffy material is justified and the chosen cores can be considered as representative of the deeper central basin. The concentrations of Mn_{diss} and total sulfide in the pore water from six cores were also determined.

The short core taken in August 2012 represented pre-MBI conditions (**Figures 2**, **5**). Sedimentary Mn/Al and Ca/Al values were elevated at ∼3 cm and showed two pronounced peaks at a sediment depth of 11–13 cm, whereas no enrichments occurred in the uppermost fluffy layer overlain by euxinic bottom waters. Mn_{diss} and sulfide increased gradually with depth in the pore water, reaching highest concentrations of 190 and 996 μM, respectively, at 20 cm depth. While sedimentary Mn and Ca enrichments at the sediment-water interface (SWI) were still absent in May 2015, elevated Mn/Al and Ca/Al values were recorded in the uppermost sediment sample in July 2015. Below a slight peak at ∼1 cm in July 2015, the pore water Mn_{diss} concentrations increased with depth, finally reaching a level comparable to that seen in the profile of the pre-MBI period. By contrast, sulfide concentrations were below the detection limit until 3 cm depth and they remained lower than those of August 2012. While surface sediment Mn/Al values in the uppermost two samples were distinctly lower in October 2015, the decline in Ca/Al was less pronounced than in the core from July 2015. Sulfide was detectable below 1 cm and Mn_{diss} levels reached a distinct near-surface maximum of >400 μM. After the second oxygenation event, around January 2016, increases in Mn/Al and Ca/Al in the uppermost sediment layer were measured in February and June 2016. Pore water sulfide levels increased further in June 2016 and Mn_{diss} still showed a near-surface maximum. Mn and Ca enrichments were absent from the surface sediments collected during the remaining two cruises, in October 2016 and March 2017, and the patterns of pore water sulfide and Mn_{diss} tended to resemble those of the pre-MBI period, represented by the August 2012 core.

Pore water fluxes of Mn_{diss} across the SWI also underwent pronounced variations (**Figure 5**). While a diffusive flux of 48 μM m^{-2} d^{-1} was determined for the pre-MBI period in August 2012, distinctly higher values were estimated for subsequent cores subjected to the MBI. Parallel to the small near-surface Mn_{diss} peak, a ∼3-fold increase in the flux occurred in July 2015. Accompanying the highest Mn_{diss} concentrations and steepest gradients was an increase in the corresponding flux, which reached a maximum of 1,253 μM m^{-2} d^{-1} in October 2015. The Mn_{diss} fluxes of the remaining three cores exhibited a decreasing trend but were still above the pre-MBI level.

Surface sediments from the short cores taken during the cruises between July 2015 and March 2017 were analyzed by SEM-EDX to elucidate the nature of the Mn enrichments. Mn oxides constituted 61% of all particles analyzed in the surface sediment from July 2015, and their morphologies were similar to those of the Mn oxides in the sediment trap (**Figures 6A–C**) and in the pelagic redoxcline of the Gotland Deep during a stagnation period (Dellwig et al., 2010, 2012). By contrast, the contribution of Mn carbonates was almost negligible. A typical Mn oxide particle contained only minor amounts of Ca, resulting in a molar Mn/Ca ratio of ∼14 (**Figure 6C**). The abundance of Mn oxides significantly decreased in October 2015, whereas Mn carbonate (Ca-rich rhodochrosite) levels increased slightly (**Figure 6D**), with a distinctly lower molar Mn/Ca ratio of < 3 due to Ca incorporation. In February 2016, the percentage of Mn oxide particles again increased, to ∼61%, while the abundance of Mn carbonate remained low. Mixed particles comprising Mn oxide and Mn carbonate were also observed, as indicated by the differing Mn/Ca ratios (**Figure 6E**). In June 2016, the abundance of Mn oxides increased, as did the abundance of Mn carbonates, to almost 7% of all particles identified (**Figure 6F**). Mixed phases appeared again, with molar Mn/Ca ratios between 2.4 and 18.9. During the last two cruises, in October 2016 and March 2017, Mn oxide particles were absent and the amount of Mn carbonate was almost negligible (**Figures 6G,H**).

Sedimentary Mn Signatures in the Gotland Deep During the Past ∼60 Years

Past Mn authigenesis in the Gotland Deep was investigated based on various geochemical parameters in the short core from August 2012. XRF scanning identified several layers enriched in Mn, especially in the lower half of the laminated sediment core (**Figure 7**). The Mn contents determined by ICP-OES in samples from a parallel core of the same cast and the Mn counts from XRF scanning generally agreed well and revealed pronounced Mn enrichments of nearly 17 wt% at a sediment depth of 10–15 cm. However, compared with the discrete samples from conventional slicing at 0.5- to 1.0-cm steps, the higher resolution of 200 μm on a 1.2-cm-wide XRF measurement line captured a clearly higher variability. This methodological difference was especially critical

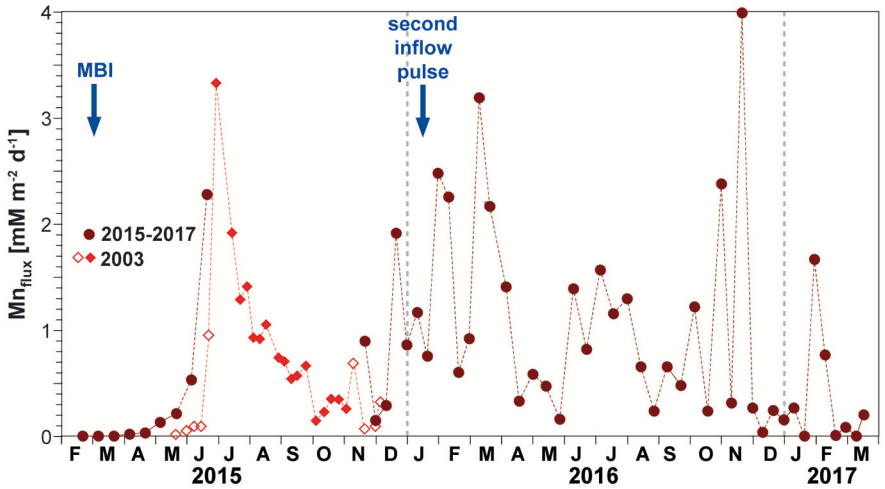

FIGURE 4 | Temporal variability of particulate Mn fluxes in a sediment trap positioned at a water depth of 186 m close to station 271 in the central Gotland Basin (brown dots: 2015–2017; open and closed red squares: 2003). Closed symbols were used for budget calculations.

for the uppermost fluffy part of the core. The slightly sloped position of the sediment material in the core liner caused a more depth-integrated sampling and prevented the registration of the two separated Mn layers, which were clearly distinguishable on the XRF scan of core depths of ∼1.5 and ∼3 cm.

A first slight increase in ^{137}Cs activity at a core depth of ∼14 cm and a peak at 11.75 cm were observed (**Figure 7**). At 9.5 cm, there was a steep rise in ^{137}Cs, with fluctuating but still elevated activities toward the core top. ^{241}Am activities were characterized by a clear maximum at a sediment depth between 14 and 11.5 cm, a single peak at 9.25 cm, and a peak between 7.75 and 8.25 cm. $^{206/207}$Pb values ranged from 1.17 to 1.21, with the lowest values at a sediment depth between ∼11 and ∼9 cm. The opal content was enriched in the topmost samples and between ∼6 and 8 cm.

DISCUSSION

Temporal Dynamics and the Fate of Mn in the Gotland Deep After the MBI of 2014

The profiles of Mn_{diss} obtained before the MBI in 2014 represent a first approximation of the conditions that prevailed during a stagnation period, that is, without the impact of substantial oxygenation events (**Figure 2**). Nonetheless, pronounced differences within the datasets were still discernible. The elevated Mn_{diss} concentrations in the bottom water in July 2006 clearly represented the remnants of the re-established euxinic conditions and the coupled reduction of deposited Mn oxides after the MBI in 2003 (Feistel et al., 2003, 2004; Turnewitsch and Pohl, 2010; Häusler et al., 2018). Conversely, the decrease in Mn_{diss} in the two lowermost samples from April 2007 was certainly due to a very short-term inflow of O_2-containing waters, documented in the time-series at site 271 (**Figures 2**, **9**; ICES, 2015). Irrespective of the rising sulfide levels in deep water, possibly attributable to a decreasing pool of reactive Fe in the sediments that exacerbated the escape of sulfide into the open water column (Lenz et al., 2015), Mn_{diss} concentrations were similar at least for the years 2008–2012 and thus suggestive of a balanced status. The Mn_{diss} level was, however, ∼2-fold higher than that in February 2015, just before the major MBI pulse of 2014 reached the Gotland Basin (**Figures 2**, **3**). The even more pronounced difference in sulfide levels can be explained by the weak oxygenation event before the major MBI, as indicated by the O_2 time series in the bottom waters from site 271 in spring 2014 (**Figure 9**; ICES, 2015). Although the average Mn_{diss} concentration in euxinic waters of 9.0 μM in August 2012 vs. 4.3 μM in February 2015 indicated substantial Mn loss, a simple inventory estimate relativizes this finding. Thus, based on the hypsography of the Gotland Basin (**Figure 9A**; Seifert and Kayser, 1995; Supplementary Dataset), the upward shift of the redoxcline by ∼10 m (**Figures 2**, **3**) significantly increased the euxinic water volume enriched in Mn, from ∼209 km^3 in 2012 to 288 km^3 in 2015. After a basin-wide extrapolation of Mn_{diss} concentrations from the water column profiles using the corresponding hypsography-based water volumes (**Figure 8**), the Mn_{diss} inventories (∼1.5 × 10^9 mol) in the euxinic water bodies were identical during the 2 years, which argues against a sustained effect of the weak pre-MBI oxygenation, at least for Mn (see Supplementary Dataset).

Increased O_2 and decreased Mn_{diss} concentrations on 3 March 2015 represented the first signals of the approaching MBI from 2014 (**Figure 3**). This date accords with an O_2 time series from a profiling mooring in the Gotland Deep (Prien and Schulz-Bull, 2016; Holtermann et al., 2017). In the following months, the main MBI phase caused the almost complete oxygenation of the water column, with only a thin remnant of the previously euxinic water body at around 120 m water depth (**Figure 3**). Correspondingly, Mn_{diss} concentrations dropped to near nanomolar levels in these oxygenated waters, thereby enhancing the formation and downward deposition of particulate Mn oxides, as documented

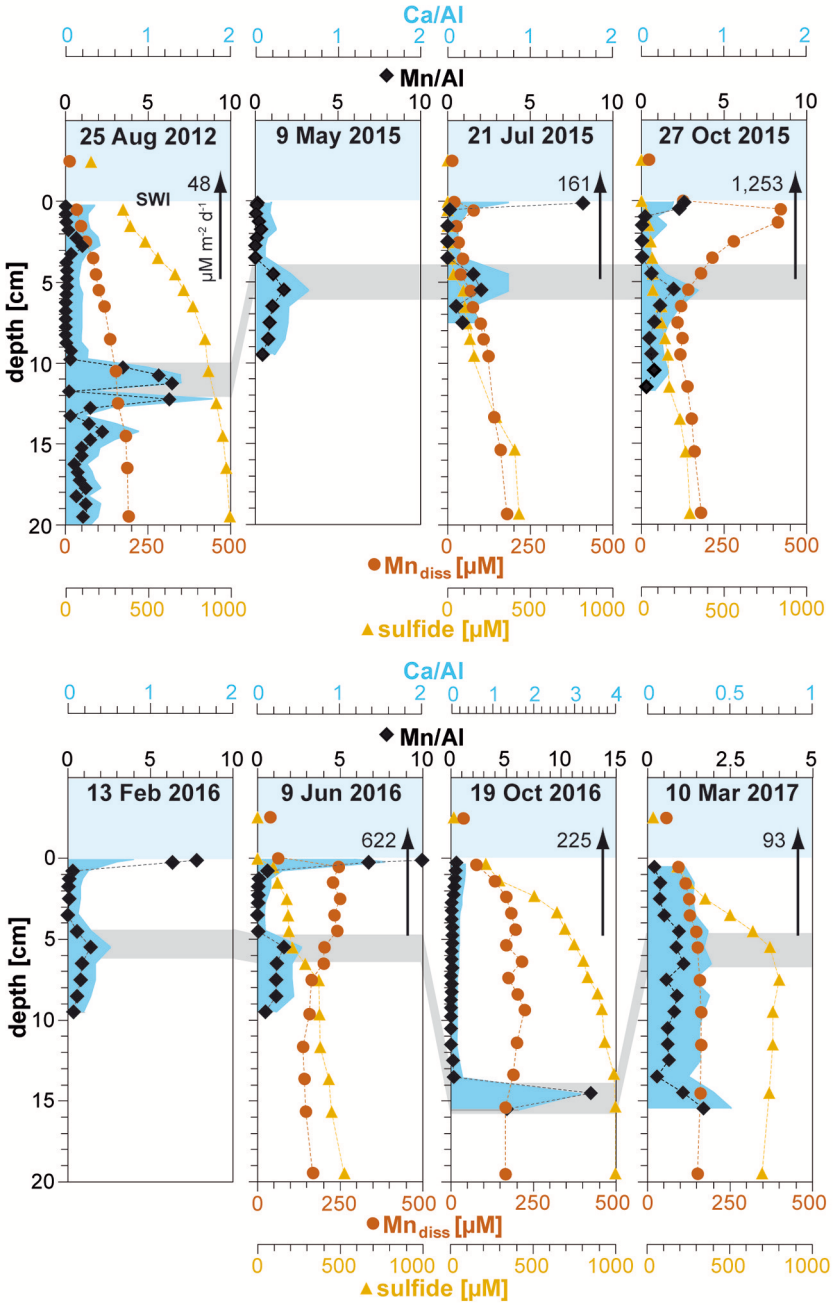

FIGURE 5 | Sedimentary Mn/Al and Ca/Al values, and Mn_{diss} and total sulfide concentrations in pore waters from short cores obtained close to station 271 in the central Gotland Basin. Numbers next to the black arrows indicate pore water fluxes of Mn_{diss} across the sediment-water interface (in $\mu M\ m^{-2}\ d^{-1}$). Gray bars indicate core parallelization based on Pb/Al ratios (Figure S3).

by the sediment trap (**Figure 4**). Although the position of the trap at a water depth of ∼186 m caused a bias between the detection of sinking Mn oxides and the onset of bottom water oxygenation, the steep increase in Mn_{part} fluxes in June 2015 reflected the considerable deposition of Mn oxides at the sediment surface. A temporal bias between the onsets of water column oxygenation and Mn oxide deposition was also apparent in the surface sediments taken close to station 271. Despite the presence of O_2 in nearly the entire water column for more than a month, there was no sign of Mn enrichment in the uppermost fluffy sediments in May 2015 (**Figure 5**). By contrast, an analysis of the core taken in July 2015 showed strongly elevated Mn/Al ratios in the uppermost sample (**Figure 5**). Particle analysis by SEM-EDX revealed a relative abundance of >60% and further supported

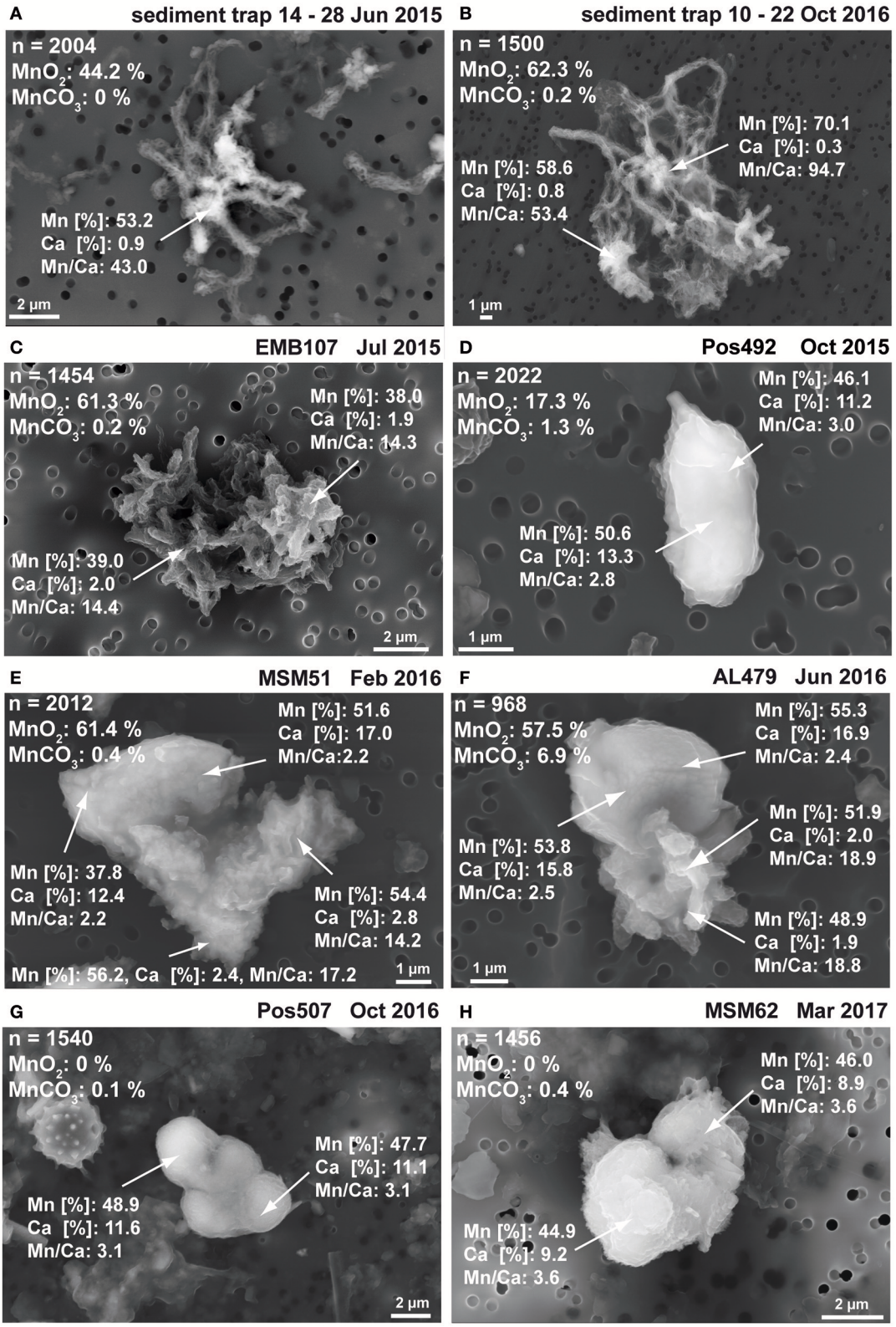

FIGURE 6 | Scanning electron microscopy with energy dispersive X-ray spectroscopy photographs and the results of particle analyses of the Mn mineral phases present in material of the sediment trap **(A, B)** and in the fluffy surface sediments **(C–H)** close to station 271 in the central Gotland Basin.

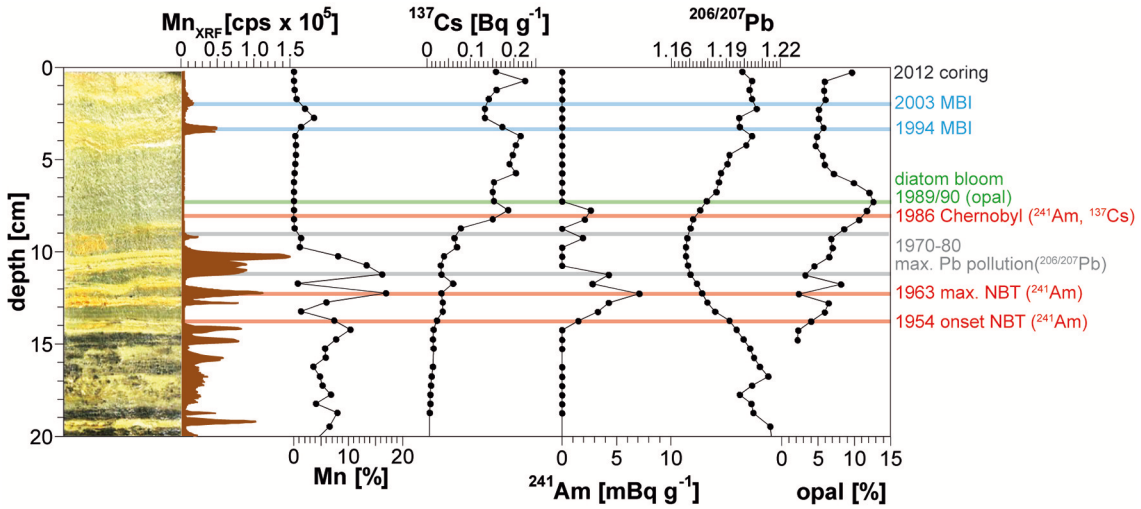

FIGURE 7 | Photograph, Mn counts (X-ray fluorescence core scanning), Mn contents (inductively coupled plasma optical emission spectrometry), activities of ^{137}Cs and ^{241}Am, $^{206/207}$Pb values, and biogenic opal contents of the short core taken in August 2012 close to station 271 in the central Gotland Basin. The data were used to identify time markers for event-stratigraphic dating of the sediment core (Supplementary Dataset).

the clear dominance of Mn oxide particles (**Figure 6C**). The similar morphologies of the Mn oxides and particles found in the sediment trap and in the pelagic redoxclines of the Baltic and Black Seas (**Figures 6A,B**; Dellwig et al., 2010) provide evidence of their origin in the water column. Because agglomeration with organic mucus reduces the density and consequently the sinking velocity of Mn oxides (<1 m d^{-1}; Glockzin et al., 2014), the elevated current velocities resulting from the intruding water masses possibly have delayed the significant deposition of these particles (Holtermann et al., 2017).

Despite the prominence of O_2 in nearly the entire water column, a first signal of the re-establishment of bottom water anoxia was already detected on 09 May 2015, by a slightly elevated Mn_{diss} concentration in the supernatant water of the short core (**Figure 3**). This shift in the bottom water redox regime was even more pronounced in the Mn_{diss} profiles from the cruises in July, September, October, and November 2015 (**Figure 3**). Elevated Mn_{diss} concentrations in the supernatant water and a peak of 81 μM in the pore water just below the Mn/Al peak at the sediment surface in July 2015 implied the onset of Mn oxide reduction and Mn_{diss} escape into the open water column (**Figures 3**, **5**). Consequently, Mn enrichment in the surface sediment decreased and a further increase in the bottom and pore water concentrations of Mn_{diss} occurred in October 2015. This liberated Mn_{diss}, however, was trapped in the bottom waters below a depth of ∼210 m, as indicated by the enhanced Mn_{part} concentrations of SPM in July and October 2015 (**Figure 3**).

The return to pronounced bottom water euxinia was interrupted by a second inflow phase that occurred between the cruises of November 2015 and February 2016. According to the ICES Dataset on Oceanography, O_2 (26 μM) first appeared, at 239 m, on 3 December 2015, (**Figure 9**), but O_2 concentrations decreased in the following cruise, to 7.6 μM, and a slight presence of ∼4 μM sulfide was even determined, on 8 January 2016. Therefore, the main onset of this second inflow pulse must have been between 8 January and 4 February 2016. While the intermediate water column in February 2016 was subjected to pronounced O_2 consumption, the intruding O_2-containing waters most likely caused an uplift of the former anoxic bottom water (**Figure 3**; Holtermann et al., 2017). The subsequent oxygenation of the water column again resulted in pronounced Mn oxide formation and deposition, as indicated by the increasing Mn_{part} fluxes in the sediment trap and the Mn_{part} enrichments in the surface sediments in February and June 2016 (**Figures 4**, **5**). Nevertheless, the rising concentrations of Mn_{diss} and sulfide in the bottom and pore waters beginning in June 2016 (**Figures 3**, **5**) again suggested a comparatively fast switch to a reducing environment in the deeper Gotland Basin. Mn_{part} concentrations as high as 2.4 μM were measured at a water depth of ∼210 m in October 2016 (**Figure 3**); however, these Mn oxides most likely dissolved in the deeper euxinic waters before reaching the seafloor, as also indicated by the absence of Mn enrichments in the corresponding surface sediments (**Figures 5**, **6**). Data from the final two cruises of February and March 2017 documented a progressive extension of euxinic bottom waters highly enriched in Mn_{diss} and the final development toward pre-MBI-like conditions (**Figures 2**, **3**).

The strong Mn_{diss} enrichments suggested a relatively rapid return to reducing near-bottom conditions within less than 3.5 months after each of the two oxygenation events. The reconstructed duration of bottom water oxygenation caused by the first inflow in winter 2014/2015 was about half as long as that determined from the instrumental O_2 time series from the deep water (below 230 m water depth) of the Gotland Basin (**Figure 9**; ICES, 2015). This difference was due to the inclusion of the supernatant water samples from the short cores in our dataset,

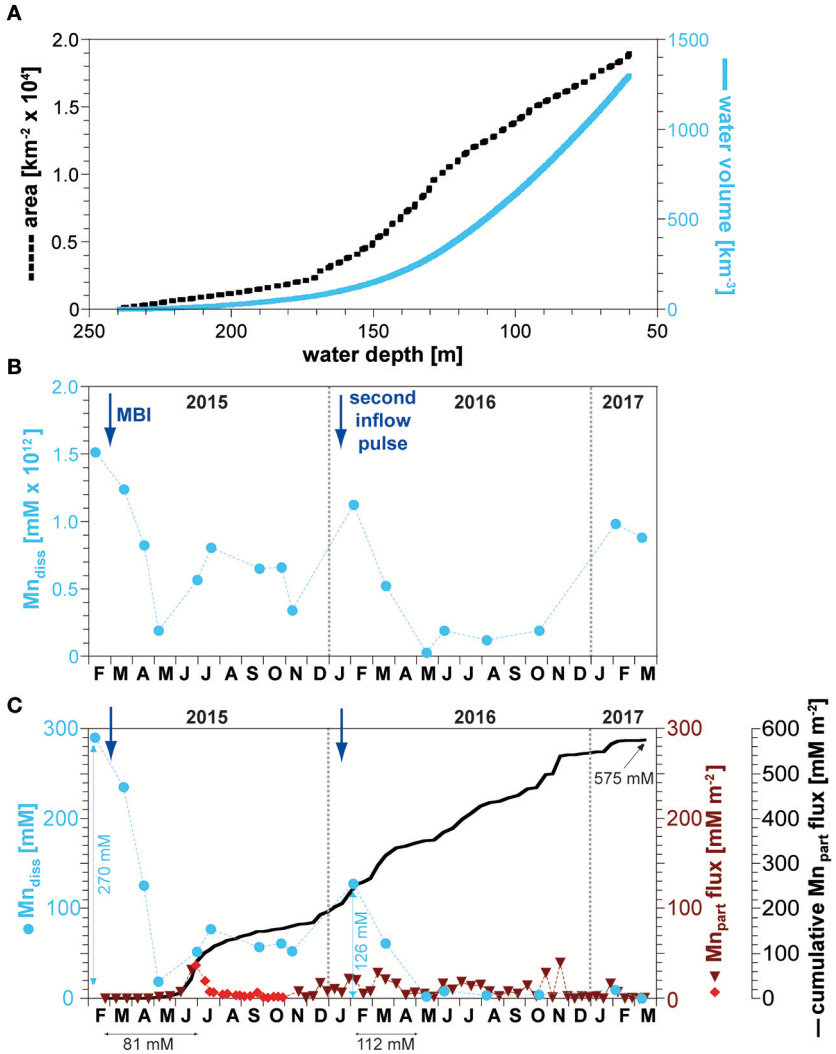

FIGURE 8 | (A) Hypsography of the Gotland Basin (Seifert and Kayser, 1995). Temporal variability of **(B)** the calculated Mn_{diss} inventories in the water column for the entire basin below a water depth of 70 m during the observation period from February 2015 until March 2017 and **(C)** comparison of Mn_{diss} inventories (blue dots) of the water body above the sediment trap (70–186 m water depth, base area 1 m^2), sum of Mn_{part} fluxes from the sediment trap for the individual sampling intervals (brown triangles: 2015–2017 red squares: 2003), and cumulative Mn_{part} flux from the sediment trap (black line, total Mn_{part} flux = 575 mM m^{-2}).

to reflect the conditions very close to the SWI. Although the MBI in 2014 was the third strongest since 1880, with a strength roughly twice as high as the previous MBI, in 2003 (Mohrholz et al., 2015), oxygenation of the Gotland Deep bottom waters was less efficient (**Figure 9**; ICES, 2015). This discrepancy was unexpected, especially given the distinctly lower sulfide level in 2015 than in 2003. Neumann et al. (2017) suggested that the larger amounts of O_2 that entered the Gotland Basin in 2003 were supported by several weaker inflows carrying additional O_2 and that the strength of an MBI is not necessarily a measure of its oxidation capacity in the deeper parts of the Baltic Sea.

Mn Balance Calculations

The water column profiles obtained in the Gotland Deep within the course of the MBI from 2014 suggest substantial losses of Mn_{diss} due to O_2 inputs and the subsequent formation of particulate Mn oxides that sank toward the sea floor (**Figures 3**, **5**, **6**). However, the relatively fast re-establishment of anoxic conditions in the pore and bottom waters also caused a reduction of deposited Mn oxides and an elevated reflux of Mn_{diss} into the water column.

Depending on the basin's topography, the water volume increases exponentially with decreasing water depth (**Figure 8A**) and concentration profiles alone cannot be used to construct elemental budgets. Nonetheless, by multiplying Mn_{diss} concentrations by the corresponding volumes of the hypsography-based water depth intervals, we calculated Mn_{diss} inventories for the entire Gotland Basin below a water depth of ∼70 m (**Figure 8B**; Supplementary Dataset). The estimates were based on the assumption that the water column profiles

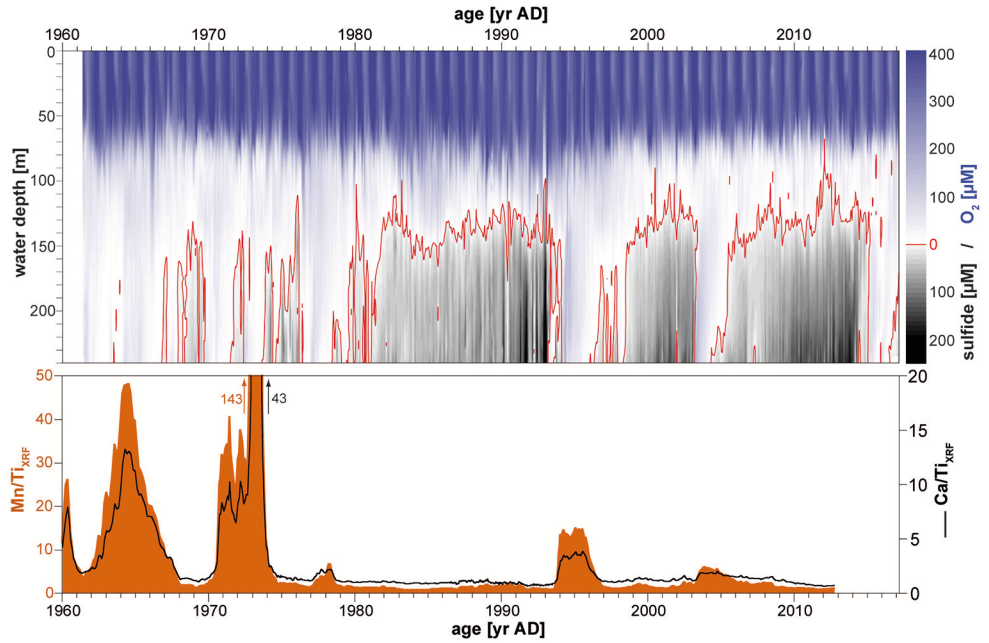

FIGURE 9 | Comparison of the instrumental time series of O_2 and total sulfide in the water column of the Gotland Deep at site 271 from 1960 to 2017 (ICES, 2015) with Mn/Ti and Ca/Ti ratios from X-ray fluorescence core scanning of a dated short core taken in August 2012.

obtained in the central deep were representative of the entire basin.

Compared with the pre-MBI situation, the inventory estimates indicated a loss of almost 90% of water column Mn_{diss} within the first 2 months after the MBI reached the Gotland Basin in the end of February 2015 (**Figure 8B**). Although the deeper parts contribute only marginally to the entire basin volume, strong Mn_{diss} enrichments in the bottom waters due to the re-establishing anoxia led to the fast recovery of the Mn_{diss} inventory, with the amounts roughly half of the pre-MBI level in the following months. Apart from the somewhat longer time span until the recharge of Mn_{diss}, a comparable behavior was also apparent after the second inflow pulse, in January 2016. The Mn_{diss} inventories from the February and March 2017 cruises, which were entirely dominated by Mn_{diss} enrichments in the deeper basin, were about two-thirds of the pre-MBI level. When considering the Mn oxides still present on surface sediments below the O_2-containing water column (above ∼170 m water depth), it is more than likely that the Mn_{diss} inventory of the Gotland Basin will further increase as euxinic conditions expand.

To allow a direct comparison between Mn_{diss} inventories and Mn_{part} fluxes from the sediment trap, Mn_{diss} inventories were also estimated for the water column above the trap (186–70 m water depth) with a base area of 1 m^2 (**Figure 8C**; Supplementary Dataset). As expected, the temporal pattern of these Mn_{diss} inventories generally resembled the total basin inventories, with two prominent phases of Mn_{diss} loss after the two inflows pulses and subsequent replenishment (**Figures 8B,C**). An exception are comparatively low Mn_{diss} values during the last two cruises in 2017 because the extension of reducing bottom waters enriched in Mn_{diss} only marginally exceeded the water depth interval considered by the inventory calculation. Compared to the Mn_{diss} inventories there was no clear relation to the Mn_{part} fluxes from the sediment trap. Thus, the delays between the increases in Mn_{part} fluxes and inflow-derived Mn_{diss} losses can be explained by slowly sinking Mn oxides particles (Glockzin et al., 2014) affected by changing hydrodynamics within the course of the inflow (Holtermann et al., 2017). In addition, the cumulative amounts of Mn_{part} found in the trap until July 2015 (81 mM) were insufficient to explain the maximum Mn_{diss} loss of ∼270 mM until May 2015. In contrast, after the second inflow pulse, Mn_{diss} loss and the cumulative Mn_{part} flux were balanced for the period between February and the end of April 2016 (**Figure 8C**). However, the total cumulative Mn_{part} flux of 575 mM m^{-2} was even twice as high as the pre-MBI Mn_{diss} inventory, which strongly argued against a simple vertical consideration of sediment trap-derived Mn_{part} fluxes.

An indication of the comparatively fast change in the bottom water toward reducing conditions causing Mn oxide dissolution came from pore water profiles that showed strong Mn_{diss} enrichments close to the SWI in October 2015 and June 2016 (**Figure 5**). This suggested that the corresponding increases in bottom water Mn_{diss} concentrations and inventories were strongly related to Mn_{diss} pore water fluxes that were distinctly higher than those prior to the MBI in 2014 (**Figures 2**, **5**). Extrapolation of the highest pore water Mn_{diss} flux of 1,253 µM m^{-2} d^{-1}, which occurred in October 2015, to the area located below a water depth of 220 m (642 km^2) and subjected to anoxic conditions resulted in an areal Mn_{diss} flux of 8×10^8 mM d^{-1}. This areal pore water flux would need ∼55 days to achieve the

calculated Mn_{diss} inventory of 4.5×10^{10} mM in the water volume below 220 m (6.6 km^3). Although this time span appears reasonable, pore water fluxes alone do not adequately explain the development of Mn_{diss} inventories especially those measured toward the end of the observation period. Even if in October 2016 and March 2017 the Mn_{diss} inventory was limited to the anoxic bottom waters below a water depth of 225 m (3.8 km^3) and 190 m (38 km^3), the time needed for the respective areal pore water fluxes (1.1×10^8 mM d^{-1} for 473 km^2 and 1.4×10^8 mM d^{-1} for 1,499 km^2) to achieve bottom water inventories of 1.3×10^8 and 8.8×10^{11} mM Mn_{diss} would have increased to 1,240 and 6,308 days, respectively. The discrepancy is undoubtedly due to the fact that the pore water fluxes determined during those two cruises in the deepest part of the basin were no longer representative of the larger basin. Along with the lack of Mn oxides at the sediment surface, the pore water profile and Mn_{diss} flux from the March 2017 cruise clearly approached pre-MBI conditions (**Figure 5**) at the deepest part of the basin. An important Mn source during these stages of the re-establishment and expansion of euxinic conditions was therefore the surface sediments from shallower water depths, where Mn oxides most likely persisted.

Several aspects strongly argue for substantial basin-internal transport of low-density Mn oxide particles (Glockzin et al., 2014) by lateral currents: (i) the temporal deviation between Mn_{diss} loss in the water column and Mn oxide sedimentation (**Figure 8C**), (ii) the rapid replenishment of the water column Mn_{diss} inventory, which cannot be explained by pore water Mn fluxes alone, (iii) the presence of Mn_{part} in oxygenated waters without a significant Mn_{diss} source, e.g., in June 2016 (**Figure 3**), (iv) the highly fluctuating pattern of Mn_{part} fluxes of the sediment trap during the second inflow phase (**Figure 4**), and (v) the discrepancy between the Mn_{diss} inventory of the water column and the Mn_{part} flux determined by the sediment trap samples (**Figure 8C**). If not already reduced by expanding euxinic waters, the enhancement of bottom currents by the MBI (Holtermann et al., 2017) most likely also re-suspended Mn oxides previously deposited in the shallower parts of the basin. Indeed, the Mn contents of the surface sediment samples from two shallower stations (MUC OD in 211 m and TrKl04 in 151 m water depth) west of site 271 (**Figure 1**) in October 2015 were 9.0and 3.1 wt%, respectively (Supplementary Dataset). The overall pathway of material transport toward the central basin finds support by several previous studies. Model results suggest an anti-clockwise direction of near-bottom currents with velocities decreasing toward the central basin (Hille et al., 2006). Along with the largest thickness of Littorina muds, the authors further report highest sedimentation rates in the deepest part of the Gotland Basin. Here, highest accumulation of TOC and heavy metals relates to physical forcing rather than biogeochemical processes (Emeis et al., 1998; Leipe et al., 2011). In addition to this physical transport of Mn_{part}, bottom currents likely also enhanced the geochemical focusing of Mn_{diss} as suggested for lakes by Schaller and Wehrli (1997).

On the other hand, Mn oxide particles may also have left the basin with the intensified deep currents during the MBI. Lower salinity in the neighboring Fårö Deep during the MBI in 2014 (Holtermann et al., 2017), however, indicate that the connection to the Gotland Basin occurred mainly via comparatively Mn-poor water masses from water intermediate depths. This has also been suggested for the downstream connection to the Landsort Deep by Häusler et al. (2018). Along with the basin's topography surrounded by sill depths of ~130 m and less, the current patterns in the deep Gotland Basin rather argue for a pronounced basin-internal cycling of Mn (Hille et al., 2006; Holtermann et al., 2017).

Implications for Mn Carbonate Formation

Although the sediments of the deep basins of the Baltic Sea are the modern type-locality for exceptional Mn carbonate accumulation (Lenz et al., 2015; Häusler et al., 2018), our data argue against prominent Mn carbonate formation, at least in the central Gotland Deep subsequent to the MBI from 2014. Studies of the influence of previous MBIs on sedimentary Mn dynamics in the Gotland Deep require dating of the sediments to correlate instrumental time series from the water column with sediment signatures. This approach was first applied by Neumann et al. (1997), who compared dated Mn carbonate records of sub-recent sediments with the hydrographic long-term data available for the Gotland Basin. However, as recently shown for Mn-rich sediments from the Landsort Deep by Häusler et al. (2018), the application of CRS-based age modeling using ^{210}Pb (Appleby and Oldfield, 1978) is strongly compromised by the ingrowth of authigenic Mn carbonate and scavenging processes at pelagic redoxclines (Wei and Murray, 1994; Swarzenski et al., 1999). To construct an age model for the short core obtained from site 271 in 2012, we used the event-stratigraphic dating method, previously successfully applied to Mn-rich sediments from the Landsort Deep (Häusler et al., 2018) and the eastern Gotland Basin (Moros et al., 2017). Several time markers were used for the linear interpolation (**Figure 7**): the radionuclides ^{137}Cs and ^{241}Am, reflecting the onset of nuclear bomb testing in 1954 and its peak in 1963, as well as the Chernobyl accident in 1986 (Koide et al., 1977; Appleby et al., 1991), stable Pb isotopes indicating maximum Pb pollution between 1970 and 1978 (Renberg et al., 2001), a basin-wide opal layer resulting from a massive diatom bloom between 1988 and 1990 (Wasmund et al., 2011; Kabel et al., 2012), and the Mn layers that formed after the MBIs in 1994 and 2003 (Moros et al., 2017).

The XRF scan of the dated short core showed two periods of strong Mn enrichment, around 1963 and 1970 (**Figure 9**). The parallel patterns of Mn/Ti and Ca/Ti were compatible with the pronounced presence of Mn carbonate (Ca-rich rhodochrosite). A comparison with instrumental O_2/sulfide data (ICES, 2015) suggested a tight relationship between Mn carbonate and O_2-containing bottom waters, in line with the widely accepted linkage between MBIs and Mn carbonate formation (Huckriede and Meischner, 1996; Neumann et al., 1997; Sternbeck and Sohlenius, 1997). The conceptual models of those studies were based on the assumption that massive Mn oxide formation caused by MBI-related bottom water oxygenation is followed by the transformation of deposited Mn oxides into Mn carbonates during the early stages of re-establishment of anoxia. However, as noted above for the MBI from 1993 (Heiser et al., 2001), MBIs do not necessarily result in substantial Mn carbonate

formation, as was the case in our corresponding core, with its less pronounced Mn enrichments following the inflows in 1976, 1993, and especially 2003 (**Figure 9**). Although minor amounts of Mn carbonate crystals were identified in the surface sediment in June 2016 (**Figure 6F**), the fluffy layers of the cores from October 2016 and March 2017 were barren of any Mn enrichments (**Figures 5**, **6**). This finding argues against sustained Mn carbonate precipitation after the MBI from 2014. The disappearance of the freshly formed Mn carbonate in the fluffy layer samples may have been related to dissolution in the undersaturated bottom waters, as suggested by Heiser et al. (2001) for the partly missing Mn carbonate layers after the MBI in 1993.

In line with previous studies in the Gotland Basin and Landsort Deep (Neumann et al., 1997; Lenz et al., 2015; Häusler et al., 2018), the appearance of discrete Mn carbonate-rich layers in the laminated sediments implied the temporal coupling of their formation to the oxygenation events. Accordingly, a dispersed precipitation from pore waters supersaturated in Mn carbonate seems less likely. Indeed, calculation of the saturation indices for Mn carbonate from pore water data of the Gotland Deep suggests undersaturation at the SWI and supersaturation not before a sediment depth of 3–10 cm (Carman and Rahm, 1997; Heiser et al., 2001; Lenz et al., 2015). Although these studies were based on pore water data obtained during stagnation periods, with Mn_{diss} concentrations similar to those measured in our August 2012 samples (**Figure 5**), the lack of a pronounced Mn carbonate presence in the surface sediments from October 2015, when pore water Mn_{diss} concentrations were even higher close to the SWI, points to a more complex mechanism of Mn carbonate formation (**Figures 5**, **6D**), especially since fundamental changes in pore water chemistry during periods of intense (∼1960 and ∼1970) and weak to absent (e.g., the MBIs of 1993, 2003, 2014) Mn carbonate formation are rather unlikely (Lenz et al., 2015). Field data as well as experimental approaches suggest kinetic reasons and an inhibition by organics and/or phosphate as limitations on the precipitation of Ca-rich Mn carbonate in the Baltic Sea (Mucci, 1988; Jakobsen and Postma, 1989; Böttcher, 1998). Böttcher (1998) mentioned a potential role for microbial mediation, as demonstrated for other authigenic mineral phases, such as apatite and dolomite (Vasconcelos et al., 1995; Schulz and Schulz, 2005; Petrash et al., 2015).

The reduction of deposited Mn oxides as the initial step in Mn carbonate formation could occur by the upwards migration of pore water sulfide (e.g., Burdige and Nealson, 1986; Yao and Millero, 1993), but competing dissimilatory Mn reduction (e.g., Lovley, 1993) has to be considered as well. Indeed, the oxygen isotope signatures of Mn carbonates from the Gotland Basin indicated microbial involvement at least during Mn oxide reduction (Neumann et al., 2002). In incubation experiments, Aller and Rude (1988) observed the formation of Mn carbonate during microbially mediated Mn oxide reduction, in which Fe sulfides served as the reductants. In addition to Mn sulfide formation, Lee et al. (2011) reported the production of Mn carbonate by the facultative anaerobic Mn-reducing bacteria *Shewanella oneidensis* MR-1 in experiments that included Mn oxide in the medium. The enormous deposition of Mn oxides at the SWI during oxygenation events in the deeps of the Baltic Sea may therefore be accompanied by a shift in the bacterial community from sulfate- to metal-reducing phyla. A role for bacterial community dynamics during the re-establishment of anoxic conditions after the MBI from 1993 was documented by Piker et al. (1998). In that study, the sulfate reduction rates in the surface sediments (0–2 cm) in May 1995 reached distinct maxima compared to the previous oxygenated state of the bottom water in June 1994. Assuming bacterial mediation, the duration of non-euxinic conditions at the SWI may be crucial for Mn carbonate formation. In other words, the too rapid re-establishment of euxinia after a single inflow, due to excess sulfide production by sulfate-reducing bacteria, may also cause an unfavorable environment for Mn-reducing phyla potentially involved in Mn carbonate formation (Lee et al., 2011). Although there have been very few measurements allowing a description of the conditions directly at the SWI, the time series of O_2 and sulfide in the water column covering the past ∼60 years (**Figure 9**) indicated a substantial difference between Mn carbonate-rich and Mn-carbonate-poor inflow periods. Along with distinctly lower sulfide levels, bottom water oxygenation was of considerably longer duration during the Mn carbonate-rich period between the 1960s and mid-1970s (around 20 MBIs; Mohrholz et al., 2015) than was the case during the sporadic inflows entering the Gotland Basin in 1993, 2003, and 2015. This temporal aspect accords with observations in the Landsort Deep, where massive Mn carbonate formations also occurred during long-lasting periods of hypoxic (slightly oxygenated) but non-euxinic bottom water conditions (Häusler et al., 2018). In contrast to the comparatively short presence of O_2 in the bottom waters after the MBI of 2014, which fostered a considerable Mn_{diss} reflux, longer-lasting oxygenation would prevent the escape of Mn to the open water column and thus ensure a high Mn abundance at the SWI.

Although ranked as the third strongest MBI since 1880 (Mohrholz et al., 2015), the inflow from 2014 is rather of short-term relevance for Gotland basin. This is especially true when considering the fast return to an euxinic situation, which paradoxically is even promoted by the inflow of O_2-containing but also highly saline waters strengthening water column stratification. Whether this episode will have a lasting effect on nutrient and trace metal budgets remains unclear so far and asks for continuing studies. For instance, the tight relation of Mn, Fe, and P at pelagic redoxclines due to formation of mixed solid phases comprising Mn oxide, Fe oxyhydroxides, and adsorbed phosphate (Dellwig et al., 2010) was also relevant during the current inflow as indicated by elevated deposition of P- and Fe-rich particles between July 2015 and June 2016 (Figure S4). However, the absence of P enrichments at the SWI during re-establishing euxinia (October 2016 and March 2017) suggests considerable release of phosphate back into the water column. While Mn carbonates incorporate certain amounts of phosphate (Jilbert and Slomp, 2013), as seen by elevated P/Al values in older Mn-rich layers below 10 cm sediment depth (**Figure 5** and Figure S4), this P sink is currently missing.

The lack of Mn carbonate not only compromises its use as an indicator for past inflow events but also has important implications for other proxies related to Mn authigenesis. A

prominent example is Mo and its isotopes, showing strong fractionation during scavenging by Mn oxides (Wasylenki et al., 2008). The possible conservation of the altered isotope signature by sedimentary fixation of Mo released from dissolving Mn oxides may therefore result in misleading redox interpretations (Noordmann et al., 2015; Kurzweil et al., 2016; Scholz et al., 2018). Complementing studies including trace metals are required to shed more light on the possible pitfalls that may be generated by inflow events like the one in 2014 because such oxygenation events should be also of relevance for other restricted basins and fjords as well as ancient epicontinental seas that were often subjected to pronounced O_2-deficiency but also redox changes (Hein et al., 1999; Jenkyns, 2010).

CONCLUSIONS

The dynamics of Mn in the water column and sediments were studied in the Gotland Deep (central Baltic Sea) subjected to an MBI of 2014. The first signals of water column oxygenation due to the approaching inflow waters appeared at the beginning of March 2015. This was followed by an estimated loss of nearly 90% of the Mn_{diss} inventory in the water column over the following 2 months, which caused a remarkable deposition of Mn oxides. However, increased Mn_{diss} pore water concentrations and fluxes as well as elevated bottom water Mn_{diss} levels suggested the re-establishment of reducing conditions at the latest after 3.5 months. A second inflow pulse in the beginning of 2016 interrupted this development, but after less than 4 months there was a shift back to reducing bottom waters as well.

Budget calculations indicated a Mn_{diss} recovery of ∼70% of the pre-MBI level at the end of the observation period in winter 2017. The recovery could not be explained by pore water fluxes from the central basin alone. Along with the Mn_{part} fluxes determined from a sediment trap, these estimates further suggested a pronounced basin-internal cycling of Mn during and subsequent to the MBI, which may have benefitted from the circulation patterns in the Gotland Basin and concomitant sediment focusing, including the transport of solid Mn phases from shallower areas toward the central deep.

A comparison of a dated sediment Mn record with instrumental O_2/sulfide data generally confirmed the close relationship between Mn carbonate and inflow-related bottom water oxygenation. However, compared to the longer-lasting oxygenation periods in the 1960s and early 1970s, the less pronounced or even absent Mn enrichments after the single inflows in 1976, 1993, and 2003 implied unfavorable conditions for Mn carbonate formation, possibly due to the too rapid shift back to euxinic conditions. Since there was no indication for substantial Mn carbonate formation after both oxygenation pulses in 2015 and 2016 within our study period of ∼2 years, it appears rather unlikely that intensive Mn carbonate formation will take place under the currently fast re-establishing euxinic situation. This assumption compromises the use of Mn carbonate layers as a simple proxy for the identification of past MBIs. For instance, scavenged trace metals imported to an increased extent by deposited Mn oxides may serve as complementing proxies if conditions at the SWI assure their fixation. Nonetheless, the combined consideration of a previous study in the Landsort Deep (Häusler et al., 2018) and the present work in the Gotland Basin emphasizes the suitability of the deeps of the Baltic Sea as modern analogs for oxygen-deficient but comparatively dynamic systems in the geological past.

AUTHOR CONTRIBUTIONS

OD designed the study, performed ICP measurements, and wrote the manuscript. BS contributed the gamma spectroscopy data. DM organized sampling during several cruises and contributed oceanographic knowledge. FP was responsible for the sediment trap. KH contributed to the age model. HA was involved in the oceanography and the age model. All authors contributed to data analysis, discussion, and finalization of the manuscript.

ACKNOWLEDGMENTS

We are indebted to the IOW cruise leaders M. Gogina, G. Jost, K. Jürgens, J. Kuss, V. Mohrholz, M. Naumann, R. Prien, M. Schmidt, L. Umlauf, J. Waniek, N. Wasmund as well as U. Lips (Tallinn University of Technology) and R. Schneider (University of Kiel) for enabling extra CTD casts, J. Donath for water sampling during monitoring cruises, and to the captains and crews of the RVs *Alkor*, *Elisabeth Mann Borgese*, *Maria S. Merian*, *Meteor*, *Poseidon*, *Prof. A. Penck*, and *Salme*. We thank R. Bahlo and S. Plewe for the SEM-EDX support, A. Köhler for the acid digestions, U. Hehl and R. Hansen for sediment trap deployment and analyses, and T. Leipe and M. Moros for MUCs from cruises MSM51 and 62. The authors thank two reviewers for constructive comments on an earlier version of the manuscript. This work was funded by the Leibniz Association through grant SAW-2017-IOW-2 649 (BaltRap) and the IOW monitoring program. The publication of this article was funded by the Open Access Fund of the Leibniz Association.

Special thanks to our bosun Dieter Knoll, who died in late 2017.

SUPPLEMENTARY MATERIAL

The Supplementary Material for this article can be found online at: https://www.frontiersin.org/articles/10.3389/fmars.2018.00248/full#supplementary-material

REFERENCES

Aller, R. C., and Rude, P. D. (1988). Complete oxidation of solid phase sulfides by manganese and bacteria in anoxic marine sediments. *Geochim. Cosmochim. Acta* 52, 751–765. doi: 10.1016/0016-7037(88)90335-3

Appleby, P. G., and Oldfield, F. (1978). The calculation of lead-210 dates assuming a constant rate of supply of unsupported ^{210}Pb to the sediment. *Catena* 5, 1–8. doi: 10.1016/S0341-8162(78)80002-2

Appleby, P. G., Richardson, N., and Nolan, P. J. (1991). ^{241}Am dating of lake sediments. *Hydrobiologia* 214, 35–42. doi: 10.1007/BF00050929

Berg, P., Risgaard-Petersen, N., and Rysgaard, S. (1998). Interpretation of measured concentration profiles in sediment pore water. *Limnol. Oceanogr.* 43, 1500–1510. doi: 10.4319/lo.1998.43.7.1500

Böttcher, M. E. (1998). Manganese(II) partitioning during experimental precipitation of rhodochrosite–calcite solid solutions from aqueous solutions. *Mar. Chem.* 62, 287–297. doi: 10.1016/S0304-4203(98)00039-5

Boudreau, B. P. (1997). *Diagenetic Models and their Implementation: Modeling Transport and Reactions in Aquatic Sediments*. Berlin; Heidelberg: Springer-Verlag.

Brady, N. C. (1984). *The Nature and Properties of Soils, 9*. New York, NY: Macmillan Publishing Co.

Brügmann, L., Hallberg, R., Larsson, C., and Löffler, A. (1998). Trace metal speciation in sea and pore water of the Gotland Deep, Baltic Sea, 1994. *Appl. Geochem.* 13, 359–368. doi: 10.1016/S0883-2927(97)00105-4

Burdige, D. J. (1993). The biogeochemistry of manganese and iron reduction in marine sediments. *Earth Sci. Rev.* 35, 249–284. doi: 10.1016/0012-8252(93)90040-E

Burdige, D. J., and Nealson, K. H. (1986). Chemical and microbiological studies of sulfide-mediated manganese reduction. *Geomicrobiol. J.* 4, 361–387. doi: 10.1080/01490458609385944

Calvert, S. E., and Pedersen, T. F. (1993). Geochemistry of recent oxic and anoxic marine sediments: implications for the geological record. *Mar. Geol.* 113, 67–88. doi: 10.1016/0025-3227(93)90150-T

Calvert, S. E., and Pedersen, T. F. (1996). Sedimentary geochemistry of manganese; implications for the environment of formation of manganiferous black shales. *Econ. Geol.* 91, 36–47. doi: 10.2113/gsecongeo.91.1.36

Calvert, S. E., and Price, N. B. (1970). Composition of manganese nodules and manganese carbonates from Loch Fyne, Scotland. *Contribut. Mineral. Petrol.* 29, 215–233. doi: 10.1007/BF00373306

Carman, R., and Rahm, L. (1997). Early diagenesis and chemical characteristics of interstitial water and sediments in the deep deposition bottoms of the Baltic proper. *J. Sea Res.* 37, 25–47. doi: 10.1016/S1385-1101(96)00003-2

Carstensen, J., Andersen, J. H., Gustafsson, B. G., and Conley, D. J. (2014). Deoxygenation of the Baltic Sea during the last century. *Proc. Natl. Acad. Sci. U.S.A.* 111, 5628–5633. doi: 10.1073/pnas.1323156111

Cline, J. D. (1969). Spectrophotometric determination of hydrogen sulfide in natural waters. *Limnol. Oceanogr.* 14, 454–458. doi: 10.4319/lo.1969.14.3.0454

Croudace, I. W., Rindby, A., and Rothwell, R. G. (2006). ITRAX: description and evaluation of a new multi-function X-ray core scanner. *Geol. Soc. Lond. Spec. Publ.*267, 51–63. doi: 10.1144/GSL.SP.2006.267.01.04

Davidson, A. T., and Marchant, H. J. (1987). Binding of manganese by Antarctic Phaeocystis pouchetii and the role of bacteria in its release. *Mar. Biol.* 95, 481–487. doi: 10.1007/BF00409577

Dellwig, O., Leipe, T., März, C., Glockzin, M., Pollehne, F., Schnetger, B. et al. (2010). A new particulate Mn-Fe-P-shuttle at the redoxcline of anoxic basins. *Geochim. Cosmochim. Acta* 74, 7100–7115. doi: 10.1016/j.gca.2010.09.017

Dellwig, O., Schnetger, B., Brumsack, H.-J., Grossart, H.-P., and Umlauf, L. (2012). Dissolved reactive manganese at pelagic redoxclines (part II): hydrodynamic conditions for accumulation. *J. Mar. Syst.* 90, 31–41. doi: 10.1016/j.jmarsys.2011.08.007

De Vitre, R. R., Buffle, J., Perretm, D., and Baudat, R. (1988). A study of iron and manganese transformations at the O2S(-II) transition layer in a eutrophic lake (Lake Bret, Switzerland): a multimethod approach. *Geochim. Cosmochim. Acta* 52, 1601–1613. doi: 10.1016/0016-7037(88)90229-3

Dahl, T. W., Anbar, A. D., Gordon, G. W., Rosing, M. T., Frei, R., and Canfield, D. E. (2010). The behavior of molybdenum and its isotopes across the chemocline and in the sediments of sulfidic Lake Cadagno, Switzerland. *Geochim. Cosmochim. Acta* 74, 144–163. doi: 10.1016/j.gca.2009.09.018

Diaz, R. J., and Rosenberg, R. (2008). Spreading dead zones and consequences for marine ecosystems. *Science* 321, 926–929. doi: 10.1126/science.1156401

Dyrssen, D., and Kremling, K. (1990). Increasing hydrogen sulfide concentration and trace metal behavior in the anoxic Baltic waters. *Mar. Chem.* 30, 193–204. doi: 10.1016/0304-4203(90)90070-S

EMODnet Bathymetry Consortium (2016). *EMODnet Digital Bathymetry (DTM)*. EMODnet Bathymetry.

Emeis, K.-C., Neumann, T., Endler, R., Struck, U., Kunzendorf, H., and Christiansen, C. (1998). Geochemical records of sediments in the Eastern Gotland Basin—products of sediment dynamics in a not-so-stagnant anoxic basin? *Appl. Geochem.* 13, 349–358. doi: 10.1016/S0883-2927(97)00104-2

Feistel, R., Nausch, G., Heene, T., Piechura, J., and Hagen, E. (2004). Evidence for a warm water inflow into the Baltic Proper in summer 2003. *Oceanologia* 46, 581–598.

Feistel, R., Nausch, G., Matthäus, W., and Hagen, E. (2003). Temporal and spatial evolution of the Baltic deep water renewal in spring 2003. *Oceanologia* 45, 623–642.

Friedl, G., Wehrli, B., and Manceau, A. (1997). Solid phases in the cycling of manganese in eutrophic lakes: new insights from EXAFS spectroscopy. *Geochim. Cosmochim. Acta* 61, 275–290. doi: 10.1016/S0016-7037(96)00316-X

Gingele, F. X., and Kasten, S. (1994). Solid-phase manganese in Southeast Atlantic sediments: implications for the paleoenvironment. *Mar. Geol.* 121, 317–332. doi: 10.1016/0025-3227(94)90037-X

Glockzin, M., Pollehne, F., and Dellwig, O. (2014). Stationary sinking velocity of authigenic manganese oxides at pelagic redoxclines. *Mar. Chem.* 160, 67–74. doi: 10.1016/j.marchem.2014.01.008

Gustafsson, B. G., Schenk, F., Blenckner, T., Eilola, K., Meier, H. E. M., Müller-Karulis, B. et al. (2017). Reconstructing the development of Baltic Sea eutrophication 1850–2006. *Ambio* 41, 534–548. doi: 10.1007/s13280-012-0318-x

Hansel, C. M. (2017). "Chapter 2: Manganese in marine microbiology," in *Advances in Microbial Physiology 70,* ed R. K. Poole (London: Academic Press), 37–83.

Hardisty, D. S., Riedinger, N., Planavsky, N. J., Asael, D., Andrén, T., Jørgensen, B. B. et al. (2016). A Holocene history of dynamic water column redox conditions in the landsort deep, Baltic Sea. *Am. J. Sci.* 316, 713–745. doi: 10.2475/08.2016.01

Häusler, K., Dellwig, O., Schnetger, B., Feldens, P., Leipe, T., Moros, M. et al. (2018), Massive Mn carbonate formation in the Landsort deep (Baltic Sea): Hydrographic prerequisites, temporal succession and Mn budget calculations. *Mar. Geol.* 395, 260–270. doi: 10.1016/j.margeo.2017.10.010

Hein, J. R., Fan, D., Ye, J., Liu, T., and Yeh, H.-W. (1999). Composition and origin of early Cambrian Tiantaishan phosphorite–Mn carbonate ores, Shaanxi province, China. *Ore. Geol. Rev.* 15, 95–134. doi: 10.1016/S0169-1368(99)00017-7

Heiser, U., Neumann, T., Scholten, J., and Stüben, D. (2001). Recycling of manganese from anoxic sediments in stagnant basins by seawater inflow: a study of surface sediments from the Gotland Basin, Baltic Sea. *Mar. Geol.* 177, 151–166. doi: 10.1016/S0025-3227(01)00129-3

Hille, S., Leipe, T., and Seifert, T. (2006). Spatial variability of recent sedimentation rates in the Eastern Gotland Basin (Baltic Sea). *Oceanologia* 48, 297–317.

Hinrichs, J., Dellwig, O., and Brumsack, H.-J. (2002). Lead in sediments and suspended particulate matter of the German Bight: natural versus anthropogenic origin. *Appl. Geochem.* 17, 621–632. doi: 10.1016/S0883-2927(01)00124-X

Hlawatsch, S., Neumann, T., van den Berg, C. M. G., Kersten, M., Harff, J., and Suess, E. (2002). Fast-growing, shallow-water ferro-manganese nodules from the western Baltic Sea: origin and modes of trace element incorporation. *Mar. Geol.* 182, 373–387. doi: 10.1016/S0025-3227(01)00244-4

Holtermann, P. L., Prien, R., Naumann, M., Mohrholz, V., and Umlauf, L. (2017). Deepwater dynamics and mixing processes during a major inflow event in the central Baltic Sea. J. *Geophys. Res. Oceans* 122, 6648–6667. doi: 10.1002/2017JC013050

Huckriede, H., and Meischner, D. (1996). Origin and environment of manganese-rich sediments within black-shale basins. *Geochim. Cosmochim. Acta* 60, 1399–1413. doi: 10.1016/0016-7037(96)00008-7

Hurrell, J. W. (1995). Decadal trends in the North Atlantic oscillation: regional temperatures and precipitation. *Science* 269, 676–679. doi: 10.1126/science.269.5224.676

ICES (2015). *Dataset on Oceanography*. Copenhagen: The International Council for the Exploration of the Sea.

Jacobs, L., Emerson, S., and Huested, S. S. (1987). Trace metal geochemistry in the Cariaco trench. *Deep Sea Res. Part A. Oceanogr. Res. Pap*. 34, 965–981. doi: 10.1016/0198-0149(87)90048-3

Jacobs, L., Emerson, S., and Skei, J. (1985). Partitioning and transport of metals across the O2H2S interface in a permanently anoxic basin: framvaren Fjord, Norway. *Geochim. Cosmochim. Acta* 49, 1433–1444. doi: 10.1016/0016-7037(85)90293-5

Jakobsen, R., and Postma, D. (1989). Formation and solid solution behavior of Ca-rhodochrosites in marine muds of the Baltic deeps. *Geochim. Cosmochim. Acta* 53, 2639–2648, doi: 10.1016/0016-7037(89)90135-X

Jenkyns, H. C. (2010). Geochemistry of oceanic anoxic events. *Geochem. Geophys. Geosyst*. 11, Q03004. doi: 10.1029/2009GC002788

Jilbert, T., and Slomp, C. P. (2013). Iron and manganese shuttles control the formation of authigenic phosphorus minerals in the euxinic basins of the Baltic Sea. *Geochim. Cosmochim. Acta* 107, 155–169. doi: 10.1016/j.gca.2013.01.005

Johnson, J. E., Webb, S. M., Ma, C., and Fischer, W. W. (2016). Manganese mineralogy and diagenesis in the sedimentary rock record. *Geochim. Cosmochim. Acta* 173, 210–231. doi: 10.1016/j.gca.2015.10.027

Kabel, K., Moros, M., Porsche, C., Neumann, T., Adolphi, F., Andersen, T. J. et al. (2012). Impact of climate change on the Baltic Sea ecosystem over the past 1,000 years. *Nat. Clim. Change* 2, 871–874. doi: 10.1038/nclimate1595

Koide, M., Goldberg, E. D., Herron, M. M., and Langway, C. C. (1977). Transuranic depositional history in south Greenland firn layers. *Nature* 269, 137–139. doi: 10.1038/269137a0

Koschinsky, A., Winkler, A., and Fritsche, U. (2003). Importance of different types of marine particles for the scavenging of heavy metals in the deep-sea bottom water. *Appl. Geochem.* 18, 693–710. doi: 10.1016/S0883-2927(02)00161-0

Kurzweil, F., Wille, M., Gantert, N., Beukes, N. J., and Schoenberg, R. (2016). Manganese oxide shuttling in pre-GOE oceans – evidence from molybdenum and iron isotopes. *Earth Planet. Sci. Lett*. 452, 69–78. doi: 10.1016/j.epsl.2016.07.013

Labrenz, M., Jost, G., and Jürgens, K. (2007). Distribution of abundant prokaryotic organisms in the water column of the central Baltic Sea with an oxic-anoxic interface. *Aquat. Microb. Ecol.* 46, 177–190. doi: 10.3354/ame046177

Lee, J. H., Kennedy, D. W., Dohnalkova, A., Moore, D. A., Nachimuthu, P., Reed, S. B. et al. (2011). Manganese sulfide formation via concomitant microbial manganese oxide and thiosulfate reduction. *Environ. Microbiol.* 13, 3275–3288. doi: 10.1111/j.1462-2920.2011.02587.x

Leipe, T., Tauber, F., Vallius, H., Virtasalo, J., Uścinowicz, S., Kowalski, N. et al. (2011). Particulate organic carbon (POC) in surface sediments of the Baltic Sea. *Geo Mar. Lett*. 31, 175–188. doi: 10.1007/s00367-010-0223-x

Lenz, C., Jilbert, T., Conley, D. J., Wolthers, M., and Slomp, C. P. (2015). Are recent changes in sediment manganese sequestration in the euxinic basins of the Baltic Sea linked to the expansion of hypoxia? *Biogeosciences* 12, 4875–4894. doi: 10.5194/bg-12-4875-2015

Lepland, A., and Stevens, R. L. (1998). Manganese authigenesis in the Landsort Deep, Baltic Sea. *Mar. Geol.* 151, 1–25. doi: 10.1016/S0025-3227(98)00046-2

Lettmann, K. A., Riedinger, N., Ramlau, R., Knab, N., Böttcher, M. E., Khalili, A. et al. (2012). Estimation of biogeochemical rates from concentration profiles: a novel inverse method. *Estuar. Coast. Shelf Sci*. 100, 26–37. doi: 10.1016/j.ecss.2011.01.012

Lovley, D. (1993). Dissimilatory metal reduction. *Annu. Rev. Microbiol.* 47, 263–284. doi: 10.1146/annurev.mi.47.100193.001403

Luther, G. W., Sundby, B., Lewis, B. L., Brendel, P. J., and Silverberg, N. (1997). Interactions of manganese with the nitrogen cycle: alternative pathways to dinitrogen. *Geochim. Cosmochim. Acta* 61, 4043–4052. doi: 10.1016/S0016-7037(97)00239-1

Madison, A. S., Tebo, B. M., and Luther, G. W. (2011). Simultaneous determination of soluble manganese(III), manganese(II) and total manganese in natural (pore)waters. *Talanta* 84, 374–381. doi: 10.1016/j.talanta.2011.01.025

März, C., Stratmann, A., Matthiessen, J., Meinhardt, A. K., Eckert, S., Schnetger, B. et al. (2011). Manganese-rich brown layers in Arctic Ocean sediments: composition, formation mechanisms, and diagenetic overprint. *Geochim. Cosmochim. Acta* 75, 7668–7687. doi: 10.1016/j.gca.2011.09.046

Matthäus, W., and Franck, H. (1992). Characteristics of major Baltic inflows—a statistical analysis. *Cont. Shelf Res.* 12, 1375–1400. doi: 10.1016/0278-4343(92)90060-W

Matthäus, W., Nehring, D., Feistel, R., Nausch, G., Mohrholz, V., and Lass, H.-U. (2008). "The inflow of highly saline water into the Baltic Sea," in *State and Evolution of the Baltic Sea 1952–2005*, eds R. Feistel, G. Nausch, and N.Wasmund (Hoboken, NJ: John Wiley and Sons), 265.

Matthäus, W., and Schinke, H. (1999). *The Influence of River Runoff on Deep Water Conditions of the Baltic Sea*. Dordrecht: Springer, 1–10.

Meier, H. E. M., and Kauker, F. (2003). Modeling decadal variability of the Baltic Sea: 2. Role of freshwater inflow and large-scale atmospheric circulation for salinity. *J. Geophys. Res*. 108:3368. doi: 10.1029/2003JC001799

Middelburg, J. J., De Lange, G. J., and van Der Weijden, C. H. (1987). Manganese solubility control in marine pore waters. *Geochim. Cosmochim. Acta* 51, 759–763. doi: 10.1016/0016-7037(87)90086-X

Mohrholz, V., Naumann, M., Nausch, G., Krüger, S., and Gräwe, U. (2015). Fresh oxygen for the Baltic Sea — an exceptional saline inflow after a decade of stagnation. *J. Mar. Syst*. 148, 152–166. doi: 10.1016/j.jmarsys.2015.03.005

Moros, M., Andersen, T. J., Schulz-Bull, D., Häusler, K., Bunke, D., Snowball, I. et al. (2017). Towards an event stratigraphy for Baltic Sea sediments deposited since AD 1900: approaches and challenges. *Boreas* 46, 129–142. doi: 10.1111/bor.12193

Mucci, A. (1988). Manganese uptake during calcite precipitation from seawater: conditions leading to the formation of a pseudokutnahorite. *Geochim. Cosmochim. Acta* 52, 1859–1868. doi: 10.1016/0016-7037(88)90009-9

Murray, J. W., Jannasch, H. W., Honjo, S., Anderson, R. F., Reeburgh, W. S., Top, Z. et al. (1989). Unexpected changes in the oxic/anoxic interface in the black sea. *Nature* 338, 411–413.

Nausch, G., Matthaus, W., and Feistel, R. (2003). Hydrographic and hydrochemical conditions in the Gotland deep area between 1992 and 2003. *Oceanologia* 45, 557–569.

Neretin, L. N., Pohl, C., Jost, G., Leipe, T., and Pollehne, F. (2003). Manganese cycling in the Gotland Deep, Baltic Sea. *Mar. Chem*. 82, 125–143. doi: 10.1016/S0304-4203(03)00048-3

Neumann, T., Christiansen, C., Clasen, S., Emeis, K.-C., and Kunzendorf, H. (1997). Geochemical records of salt-water inflows into the deep basins of the Baltic Sea. *Cont. Shelf Res*. 17, 95–115. doi: 10.1016/0278-4343(96)00023-4

Neumann, T., Heiser, U., Leosson, M. A., and Kersten, M. (2002). Early diagenetic processes during Mn-carbonate formation: evidence from the isotopic composition of authigenic Ca-rhodochrosites of the Baltic Sea. *Geochim. Cosmochim. Acta* 66, 867–879. doi: 10.1016/S0016-7037(01)00819-5

Neumann, T., Radtke, H., and Seifert, T. (2017). On the importance of major Baltic inflows for oxygenation of the central Baltic Sea. *J. Geophys. Res. Oceans* 122, 1090–1101. doi: 10.1002/2016JC012525

Noordmann, J., Weyer, S., Montoya-Pino, C., Dellwig, O., Neubert, N., Eckert, S. et al. (2015). Uranium and molybdenum isotope systematics in modern euxinic basins: case studies from the central Baltic Sea and the Kyllaren fjord (Norway). *Chem. Geol.* 396, 182–195. doi: 10.1016/j.chemgeo.2014.12.012

Nyame, F. K., Beukes, N. J., Kase, K., and Yamamoto, M. (2003). Compositional variations in manganese carbonate micronodules from the lower proterozoic Nsuta deposit, Ghana: product of authigenic precipitation or post-formational diagenesis? *Sed. Geol*. 154, 159–175. doi: 10.1016/S0037-0738(02)00128-8

Petrash, D. A., Lalonde, S. V., González-Arismendi, G., Gordon, R. A., Méndez, J. A., Gingras, M. K. et al. (2015). Can Mn–S redox cycling drive sedimentary dolomite formation? A hypothesis. *Chem. Geol.* 404, 27–40. doi: 10.1016/j.chemgeo.2015.03.017.

Piker, L., Schmaljohann, R., and Imhoff, J. F. (1998). Dissimilatory sulfate reduction and methane production in Gotland deep sediments (Baltic Sea) during a transition period from oxic to anoxic bottom water (1993-1996). *Aquat. Microb. Ecol*. 14, 183–193. doi: 10.3354/ame014183

Pohl, C., and Hennings, U. (1999). The effect of redox processes on the partitioning of Cd, Pb, Cu, and Mn between dissolved and particulate phases in the Baltic Sea. *Mar. Chem*. 65, 41–53. doi: 10.1016/S0304-4203(99)00009-2

Pedersen, T. F., and Price, N. B. (1982). The geochemistry of manganese carbonate in Panama Basin sediments. *Geochim. Cosmochim. Acta* 46, 59–68. doi: 10.1016/0016-7037(82)90290-3

Prien, R. D., and Schulz-Bull, D. E. (2016). Technical note: GODESS—a profiling mooring in the Gotland Basin. *Ocean Sci.* 12, 899–907. doi: 10.5194/os-12-899-2016

Pruysers, P. A., de Lange, G. J., Middelburg, J. J., and Hydes, D. J. (1993). The diagenetic formation of metal-rich layers in sapropel-containing sediments in the eastern Mediterranean. *Geochim. Cosmochim. Acta* 57, 527–536. doi: 10.1016/0016-7037(93)90365-4

Renberg, I., Bindler, R., and Brännvall, M.-L. (2001). Using the historical atmospheric leaddeposition record as a chronological marker in sediment deposits in Europe. *Holocene* 11, 511–516. doi: 10.1191/095968301680223468

Rudnick, R. L., and Gao, S. (2003). 3.01 – "Composition of the Continental Crust," in *Treatise on Geochemistry*, ed K. K Turekian (Oxford: Pergamon), 1–64.

Schaller, T., and Wehrli, B. (1997). Geochemical-focusing of manganese in lake sediments – an indicator of deep-water oxygen conditions. *Aquat. Geochem.* 2, 359–378. doi: 10.1007/BF00115977

Schinke, H., and Matthäus, W. (1998). On the causes of major Baltic inflows - an analysis of long time series. *Cont. Shelf Res.* 18, 67–97. doi: 10.1016/S0278-4343(97)00071-X

Schnetger, B., and Dellwig, O. (2012). Dissolved reactive manganese at pelagic redoxclines (part I): a method for determination based on field experiments. *J. Mar. Syst.* 90, 23–30. doi: 10.1016/j.jmarsys.2011.08.006

Scholz, F., Baum, M., Siebert, C., Eroglu, S., Dale, A. W., Naumann, M. et al. (2018). Sedimentary molybdenum cycling in the aftermath of seawater inflow to the intermittently euxinic Gotland Deep, central Baltic Sea. *Chem. Geol.* 491, 27–38. doi: 10.1016/j.chemgeo.2018.04.031

Schulz, H. D. (2006). "Quantification of early diagenesis: dissolved constituents in marine pore water," in *Marine Geochemistry,* eds H. D. Schulz and M. Zabel (Berlin; Heidelberg: Springer), 85–128.

Schulz, H. N., and Schulz, H. D. (2005). Large sulfur bacteria and the formation of phosphorite. *Science* 307, 416–418. doi: 10.1126/science.1103096

Seeberg-Elverfeldt, J., Schlüter, M., Feseker, T., and Kölling, M. (2005). Rhizon sampling of porewaters near the sediment-water interface of aquatic systems. *Limnol. Oceanogr. Methods* 3, 361–371. doi: 10.4319/lom.2005.3.361

Seifert, T., and Kayser, B. (1995). A high resolution spherical grid topography of the Baltic Sea. *Mar. Sci. Rep.* 9, 72–88.

Skei, J. M. (1988). Formation of framboidal iron sulfide in the water of a permanently anoxic fjord - Framvaren, South Norway. *Mar. Chem.* 23, 345–352. doi: 10.1016/0304-4203(88)90103-X

Spencer, D. W., and Brewer, P. G. (1971). Vertical advection diffusion and redox potentials as controls on the distribution of manganese and other trace metals dissolved in waters of the Black Sea. *J. Geophys. Res.* 76, 5877–5892. doi: 10.1029/JC076i024p05877

Sternbeck, J., and Sohlenius, G. (1997). Authigenic sulfide and carbonate mineral formation in Holocene sediments of the Baltic Sea. *Chem. Geol.* 135, 55–73. doi: 10.1016/S0009-2541(96)00104-0.

Strady, E., Pohl, C., Yakushev, E. V., Krüger, S., and Hennings, U. (2008). Pump-CTD-System for trace metal sampling with a high vertical resolution. A test in the Gotland Basin, Baltic Sea. *Chemosphere* 70, 1309–1319. doi: 10.1016/j.chemosphere.2007.07.051

Suess, E. (1979). Mineral phases formed in anoxic sediments by microbial decomposition of organic matter. *Geochim. Cosmochim. Acta* 43, 339–352. doi: 10.1016/0016-7037(79)90199-6

Swarzenski, P. W., McKee, B. A., Sørensen, K., and Todd, J. F. (1999). ^{210}Pb and ^{210}Po, manganese and iron cycling across the O_2/H_2S interface of a permanently anoxic fjord: framvaren, Norway. *Mar. Chem.* 67, 199–217. doi: 10.1016/S0304-4203(99)00059-6.

Taylor, G. T., Iabichella, M., Ho, T.-Y., Scranton, M. I., Thunell, R. C., Muller-Karger, F. et al. (2001). Chemoautotrophy in the redox transition zone of the Cariaco Basin: a significant midwater source of organic carbon production, *Limnol. Oceanogr.* 46,148–163. doi: 10.4319/lo.2001.46.1.0148

Tebo, B. M., Bargar, J. R., Clement, B. G., Dick, G. J., Murray, K. J., Parker, D. et al. (2004). Biogenic manganese oxides: properties and mechanisms of formation. *Annu. Rev. Earth Planet. Sci.* 32, 287–328. doi: 10.1146/annurev.earth.32.101802.120213

Trouwborst, R. E., Clement, B. G., Tebo, B. M., Glazer, B. T., and Luther, G. W. III. (2006). Soluble Mn(III) in suboxic zones. *Science* 313, 1955–1957. doi: 10.1126/science.1132876

Turnewitsch, R., and Pohl, C. (2010). An estimate of the efficiency of the iron- and manganesedriven dissolved inorganic phosphorus trap at an oxic/euxinic water column redoxcline. *Glob. Biogeochem. Cycles* 24, GB4025. doi: 10.1029/2010GB003820

Vasconcelos, C., McKenzie, J. A., Bernasconi, S., Grujic, D., and Tiens, A. J. (1995). Microbial mediation as a possible mechanism for natural dolomite formation at low temperatures. *Nature* 377, 220–222. doi: 10.1038/377220a0

Wasmund, N., Tuimala, J., Suikkanen, S., Vandepitte, L., and Kraberg, A. (2011). Long-term trends in phytoplankton composition in the western and central Baltic Sea. *J. Mar. Syst.* 87, 145–159. doi: 10.1016/j.jmarsys.2011.03.010

Wasylenki, L. E., Rolfe, B. A., Weeks, C. L., Spiro, T. G., and Anbar, A. D. (2008). Experimental investigation of the effects of temperature and ionic strength on Mo isotope fractionation during adsorption to manganese oxides. *Geochim. Cosmochim. Acta* 72, 5997–6005. doi: 10.1016/j.gca.2008.08.027

Wegwerth, A., Eckert, S., Dellwig, O., Schnetger, B., Severmann, S., Weyer, S. et al. (2018). Redox evolution during Eemian and Holocene sapropel formation in the black sea. *Palaeogeogr. Palaeoclimatol. Palaeoecol.* 489, 249–260. doi: 10.1016/j.palaeo.2017.10.014

Wei, C.-L., and Murray, J. W. (1994). The behavior of scavenged isotopes in marine anoxic environments: ^{210}Pb and ^{210}Po in the water column of the Black Sea. *Geochim. Cosmochim. Acta* 58, 1795–1811. doi: 10.1016/0016-7037(94)90537-1

Yao, W., and Millero, F. J. (1993). The rate of sulfide oxidation by δMnO_2 in seawater. *Geochim. Cosmochim. Acta* 57, 3359–3365. doi: 10.1016/0016-7037(93)90544-7

Yigiterhan, O., Murray, J. W., and Tugrul, S. (2011). Trace metal composition of suspended particulate matter in the water column of the Black Sea. *Mar. Chem.* 126, 207–228. doi: 10.1016/j.marchem.2011.05.006

Zeitzschel, B., Diekmann, P., and Uhlmann, L. (1978). A new multisample sediment trap. *Mar. Biol.* 45, 285–288. doi: 10.1007/BF00391814

Zillén, L., Conley, D. J., Andrén, T., Andrén, E., and Björck, S. (2008). Past occurrences of hypoxia in the Baltic Sea and the role of climate variability, environmental change and human impact. *Earth Sci. Rev.* 91, 77–92. doi: 10.1016/j.earscirev.2008.10.001

Zopfi, J., Ferdelman, T. G., Jørgensen, B. B., Teske, A., and Thamdrup, B. (2001). Influence of water column dynamics on sulfide oxidation and other major biogeochemical processes in the chemocline of Mariager Fjord (Denmark). *Mar. Chem.* 74, 29–51. doi: 10.1016/S0304-4203(00)00091-8.

Conflict of Interest Statement: The authors declare that the research was conducted in the absence of any commercial or financial relationships that could be construed as a potential conflict of interest.